Giant dipole resonance in nuclei of the 1*p* shell. Configuration splitting and cluster effects

B. S. Ishkhanov, I. M. Kapitonov, and V. G. Neudachin

Scientific-Research Institute for Nuclear Physics, Moscow State University

R. A. Éramzhyan

Joint Institute for Nuclear Research, Dubna

Fiz. Elem. Chastits At. Yadra **12**, 905–961 (July–August 1981)

A universal property of dipole resonance in light nuclei, called configuration splitting, is established and analyzed on the basis of a great deal of experimental and theoretical work. The phenomenon consists of the occurrence of two groups of transitions which are separated in energy and formed by nucleons of different shells. The splitting is about 10 MeV in nuclei of the 1*p* shell. The phenomenon is due to the important part played by Majorana forces in light nuclei. Experiments that permit the detection of configuration splitting are described. The splitting is manifested in many phenomena associated with the excitation and subsequent decay of dipole resonance states, in particular, in photonuclear reactions, electron scattering, μ capture, radiative capture of π mesons, and in the states of hypernuclear systems.

PACS numbers: 24.30.Cz

INTRODUCTION

The most striking feature of reactions in which γ rays are absorbed by nuclei is the excitation of a giant resonance. Photonuclear resonance is primarily associated with dipole transitions. In medium and heavy nuclei, it is localized in the energy range from 13 to 18 MeV. If the nuclei are spherical, the dipole resonance in experiments with moderate energy resolution is manifested as a comparatively narrow single peak; in deformed nuclei, it is split into two. In light nuclei, an entirely different picture is observed—the resonance is spread over a broad energy region, extending almost to 40 MeV, and even in experiments with low energy resolution it takes the form of several rather broad maxima.

A theoretical interpretation of the giant photonuclear resonance for medium and heavy nuclei based on hydrodynamic notions, the so-called macroscopic approach, was given by Migdal[1] and Goldhaber and Teller.[2] The foundations of a microscopic approach, based on the shell model, were laid by Wilkinson.[3] The decisive step in this direction was made at the beginning of the sixties by Brown,[4] who introduced the concept of a collective dipole state. The real existence of such a state was demonstrated for the first time by Balashov *et al.*[5] Thus, an understanding of the collective nature of the giant resonance was achieved, and this made it possible to establish a connection between the microscopic and the collective (hydrodynamic) theories of the photoeffect.

Detailed microscopic calculations of the photonuclear dipole resonance in medium and heavy nuclei have only recently been made possible by the application of powerful computers. The results of these investigations, which reflect the latest achievements, are discussed in the review papers of Refs. 6–8.

At the beginning of the sixties, i.e., at almost the same time as the foundations of the microscopic approach were laid, it was shown that in light nuclei a single dipole state is not formed,[9–12] and it was shown[9,13] that this is because Majorana forces play an important part in light nuclei. The first consequence of this is the existence of a supermultiplet structure in light nuclei and a clearly expressed "fouring" of the nucleons (large binding energy of a nucleon if its separation destroys a closed row of the orbital Young tableau). A second consequence is that the binding energy of a closed-shell nucleon which participates in the formation of the giant resonance increases rather rapidly with increasing number of particles in the outer unfilled shell, whereas the binding energy of a nucleon on the Fermi surface, where the nucleon from the closed shell arrives, remains approximately constant. The excited states with different Young tableaux are displaced in energy so strongly that the nondiagonal part of the particle–hole interaction amplitude is too small to overcome the influence of the large spread of the energies and form a single maximum of the dipole absorption.

The resulting effect is as follows: a) the transitions from the closed shell are displaced to higher energies relative to the transitions from the outer open shell; b) the transitions from each shell are also grouped with respect to the energy, depending on the Young tableau of the resulting state.

This influence of the Majorana forces, which leads to a splitting of the dipole-absorption curve in light nuclei, has been called *configuration splitting*.[14,15]

Simultaneously, it was established theoretically that one of the clear consequences of the configuration splitting of the resonance in 1*p*-shell nuclei is the presence of very unusual decay channels of the resonance.[9–12] The theory predicted[9–11] that in the lithium isotopes the main decay channels for a highly excited ($E^* \approx 30$ MeV) nucleus should be into three or four comparatively low-energy fragments. This is a so-called *star decay*, corresponding to photodisintegration of a virtual α particle in the nucleus. Also pre-

 0090-4759/81/040362-24$02.80

dicted was a two-particle channel corresponding to fission into two equal parts: $^3He-^3H$ in ^6Li and $^4He-^3H$ in ^7Li. These predictions stimulated many experiments, which were made by Leningrad physicists.[16-19] These led to the experimental detection of star decays in ^6Li and ^7Li.

Subsequent analysis showed that the conditions for the occurrence of configuration splitting are also satisfied for nuclei in which the $2s-2d$ shell is filled.[20] This stimulated extensive experimental investigations[21-24] at the Scientific-Research Institute of Nuclear Physics at Moscow State University, and these, in conjunction with the theoretical studies,[25,11] led to the discovery of the phenomenon in the region of nuclei $24 \leq A \leq 32$. The configuration splitting is detected mainly through its specific property—highly excited states formed by transition of a nucleon from a closed shell to the valence shell, the states remaining largely uncollectivized, so that they decay, emitting low-energy nucleons, with the consequence that the nucleus $A-1$ remains comparatively highly excited (hole in the closed shell).

In the following years it was established that the excitation of giant-resonance states is not restricted to electromagnetic interactions. Having originated in the physics of photonuclear reactions, the resonance mechanism was later proposed as the dominant mechanism of muon absorption by nuclei and, later, radiative capture of π mesons.[26] This concept is penetrating further and further into other regions of medium-energy physics. A dominant role of such states in numerous meson–nucleus interaction processes has now been convincingly demonstrated.

In many processes at medium energies the dominant transitions are of dipole type[26] On the basis of this, it was shown that the phenomenon of configuration splitting of the giant resonance is also important in the interaction of mesons with light nuclei.[27-30] As in the photonuclear reactions, it is manifested through the many-particle nature of the decay in the lightest nuclei of the $1p$ shell.[31-33] However, whereas the configuration splitting is "eliminated" in photonuclear reactions in nuclei of medium mass by the residual interaction between the nucleons in the nuclei, it can be traced[34,35] much further in meson–nucleus interactions—up to nuclei with atomic number $A \approx 100$ and higher. The reason for this is that in meson–nucleus interactions a decisive part is played by spin excitations, i.e., strong nucleon transitions of the type $j^{\pi} - j'^{\pi+1}$, where, for example, j and j' can take the values $j = l + \frac{1}{2}$ and $j' = (l+1) + \frac{1}{2}$ or $j = l + \frac{1}{2}$ and $j' = (l+1) - \frac{1}{2}$, etc. As a result, in contrast to the ordinary giant dipole resonance, the energy of the spin–orbit splitting determines, as one of the most important factors, a broad spread of the particle–hole levels already in the zeroth approximation, i.e., before allowance is made for the nondiagronal matrix elements. Therefore, the corresponding states are collectivized by mixing of the particle–hole states much more weakly than the ordinary dipole excitations, so that the conditions for manifestation of configuration splitting are favorable for medium nuclei as well.

Recently, it has been shown that a supermultiplet structure of the levels is also manifested in the lightest hypernuclei of the $1p$ shell: $^6_\Lambda Li$, $^7_\Lambda Li$, and $^8_\Lambda Be$. This structure of these systems leads to interesting consequences in strangeness-changing (K^-, π^-) processes,[36] in which configuration splitting is also observed.

Thus, in all the considered phenomena we are concerned in the first place with features in the spectrum of the particle–hole energies in the zeroth approximation, i.e., before allowance is made for the nondiagonal part of the particle–hole interaction amplitude, which, under favorable circumstances, leads to collectivization of the dipole states. In this field, the development of nuclear physics has taken an unexpected turn. It would seem that the simplest aspects of the problem—the zeroth-approximation effects—have revealed important, previously uninvestigated features, thereby stimulating considerably the general level of photonuclear investigations. We now have the possibility of both "ordinary" situations with strongly collectivized dipole states in medium and heavy nuclei and situations in which the dipole absorption is distributed over a broad energy band of weakly collectivized particle–hole states. This variety in the properties of the particle–hole states is important in many problems, and this interesting inner unity of a fairly large group of phenomena has prompted us to write the present review. We discuss here qualitatively the prerequisites for the occurrence of configuration splitting and the extent to which they are present in different nuclei; the possible effects directly associated with such splitting that can serve as indicators of it; and also the results of extensive calculations and experimental investigations of this phenomenon in nuclei of the $1p$ shell.

1. PREREQUISITES FOR THE OCCURRENCE OF CONFIGURATION SPLITTING OF DIPOLE RESONANCE IN LIGHT NUCLEI AND ITS CHARACTERISTIC MANIFESTATIONS (QUALITATIVE TREATMENT)

Supermultiplet structure of light nuclei and its manifestation states forming the dipole resonance. The Majorana forces $M = -V_M \sum P^x_{ij}$ determine the basic features of the structure of light nuclei, in which a supermultiplet level scheme is realized approximately. Here, P^x_{ij} is the operator of permutation of the spatial coordinates of the nucleons; the effective value of V_M is $\langle V_M \rangle \approx 3-4$ MeV. The Young tableau $[\lambda]$ of the orbital symmetry is, as a good quantum number, the main characteristic of such structure.[37] Within one Young tableau, there can be strong mixing of the states with respect to both the orbital angular momentum L and the spin S.

There is a large energy gap between states corresponding to different Young tableaux. We shall illustrate this by taking the example of the nuclei ^6Li and ^7Li, in which the effect is most strongly manifested. Thus, in ^6Li the levels with the Young scheme [42] and configuration $0s^4 1p^2$, and in ^7Li with tableau [43] and configuration $0s^4 1p^3$, are situated in the energy range from 0 to 6 MeV, and those with the tableaux [411] in

^{6}Li and [421] in ^{7}Li from 10 to 18 MeV.[38] The situation is similar in other $1p$-shell nuclei. In even–even nuclei with $N=Z$ a large gap also arises between the lowest states with isospins $T=0$ and $T=1$, since they belong to different Young tableaux. In the first case, we have a configuration with an unbroken quadruplet in the Young tableau, for example, $0s^4 1p^4$[44] in ^{8}Be or $0s^4 1p^8$[444] in ^{12}C; in the second case, we have a configuration with broken quadruplet: $0s^4 1p^4$[431] and $0s^3 1p^8$[4431]. In nuclei of the $1p$ shell, the gap is about 15 MeV, while in the $2s-2d$ shell it is about 9 MeV. This is the fouring effect referred to above.

In describing dipole resonance in light nuclei, one usually assumes that it is formed by two groups of nucleon transitions: from a closed (inner) to a partly filled outer (or, as it is sometimes called, *valence*) shell (group B) and from a partly filled shell to an empty shell (group A). These groups are formed by $0s \to 1p$ and $1p \to (2s$ or $2d)$ transitions in nuclei of the $1p$ shell:

$$0s^4 1p^{A-4} \to \begin{cases} 0s^4 1p^{A-5}(2s \text{ or } 2d)^1 & \text{A (1a)} \\ 0s^3 1p^{A-3} & \text{B (1b)} \end{cases}$$

and $1p \to (2s$ or $2d)$ and $(2s$ or $2d) \to (3f$ or $3p)$ transitions in nuclei of the $2s-2d$ shell:

$$0s^4 1p^{12}(2s-2d)^{A-16} \to \begin{cases} 0s^4 1p^{12}(2s-2d)^{A-17}(3f \text{ or } 3p)^1 & \text{A (2a)} \\ 0s^4 1p^{11}(2s-2d)^{A-15}. & \text{B (2b)} \end{cases}$$

The dipole resonance states are to a strong degree subject to the influence of the supermultiplet structure of the low-lying states. We shall illustrate this by the example of the same nuclei ^{6}Li and ^{7}Li. In the supermultiplet scheme,[1)] the ^{6}Li ground state corresponds to the configuration $0s^4 1p^2$[42], and the ^{7}Li ground state to the configuration $0s^4 1p^3$[43]. In these two nuclei, the dipole resonance is formed basically from the states described by the configurations given in Table I. Transitions from the closed $0s$ shell (group B) are strongly displaced in energy relative to the transitions from the $1p$ shell. This is due to the fact that in nuclei in which the $1p$ shell is only beginning to be filled breakup of the quadruplet of nucleons does not occur in the transitions of group A, whereas it does in the other transitions, as can be seen from Table I. The transitions of group B are also displaced relative to one another, which is due to the gap between the states with the Young tableaux [33] and [321].

The nondiagonal part of the residual interaction of the nucleons in the nucleus is incapable of combining such widely spread levels into a single collective maximum. Moreover, because of the large energy spread the mixing of the states between these groups when allowance is made for the nondiagonal part of the interaction will be small, and they effectively retain their individuality. Therefore, the diagonal approximation (in which the energy of each state from which the resonance is formed is calculated with allowance

TABLE I. Configurations that participate in the formation of the dipole resonance in the nuclei ^{6}Li and ^{7}Li.

^{6}Li	^{7}Li
1. $0s^4 1p(2s$ or $2d)$ [411] 2. $0s^3 1p^3$ [33] 3. $0s^3 1p^3$ [321]	1. $0s^3 1p^4$ [43] 2. $0s^4 1p^2(2s$ or $2d)$ [421] 3. $0s^3 1p^4$ [331]

for only the diagonal part of the effective nucleon–nucleon interaction and without allowance for mixing of the states) can already serve as a good basis for establishing the gross structure of the dipole resonance. It was in this approximation that the first calculations were made,[9-12] and it was predicted on their basis that the dipole states in the Li isotopes are concentrated in the energy intervals $\Delta E_1 = 10-15$ MeV, $\Delta E_2 = 15-20$ MeV, and $\Delta E_3 \gtrsim 25$ MeV, respectively. Since the last maximum is associated with the breakup of a closed quadruplet in the Young tableau, it was called a maximum of quasi-α-particle absorption of γ rays. Detailed calculations made with allowance for configuration mixing[28,39,40] confirmed that the effect of this mixing is small and that each of the maxima can be unambiguously associated with a definite configuration in Table I. As early as 1963, there were experimental data[41] which indicated that in ^{6}Li there is indeed a well-formed high-energy maximum of quasi-α-particle absorption.

In nuclei in which the $1p$ shell is almost half filled, i.e., beginning with ^{8}Be, the formation of the dipole resonance already involves the breakup of a quadruplet of nucleons in the $1p$ shell. Therefore, transitions of group A are also displaced relative to each other through the manifestation of the supermultiplet structure. In the nuclei ^{9}Be and ^{13}C there will be transitions to states described by the Young tableaux with unbroken quadruplets [441] and [4441], respectively. Such states are situated very low. The corresponding low-energy branch has been called the pigmy resonance.[42]

The fouring effect of the nucleons leads to a kind of quasi-α-molecular structure of the light nuclei, which is well expressed in nuclei in the region from ^{5}He to ^{9}Be and somewhat less clearly in the remaining $1p$-shell nuclei. This effect can be interpreted as repulsion due to Majorana forces between filled rows in the Young tableau (orbital). As was shown by Brink,[43] this quasimolecular structure can be described in the framework of the multicenter Hartree–Fock method,[44] in which each orbital in the wave function is a sum of states localized with respect to different α centers.

We consider as an example the nucleus ^{9}Be. We form the molecular orbitals $\sigma_g(1p)$ and $\sigma_u(1p)$ for a $1p$ nucleon in the field of each of two α centers.[43,45] These orbitals become degenerate with respect to the energy if the centers are separated adiabatically. When the centers are brought together, the orbitals go over into $1p$ and $2s$ states, respectively. The distance between these states is only 1.7 MeV, which is much less than the oscillator frequency $\hbar\omega \approx 16$ MeV for these nuclei. Thus, even at very low energies a pigmy-res-

[1)] The admixture in the ground state of other components due to the circumstance that the Young tableau is not a strictly conserved quantity is less than 10% in these nuclei.[38]

onance dipole state arises. In the shell model, as noted above, this is the state $0s^4 1p^4 2s[441]$ with unbroken nucleon quadruplet. This effect is due to the circumstance that in the nucleus ^{9}Be it is very difficult to move the α associations apart appreciably.[37] It is therefore no surprise that the dipole-absorption curve for the nucleus ^{9}Be is closely related to that for an α particle[46] (see below). Since nucleon associations in the Li and Be isotopes are well formed, it must be borne in mind that shell calculations of the giant resonance for these nuclei somewhat over estimate the part played by "fermization" of the system of A nucleons, i.e., the part played by antisymmetrization between the clusters.

In nuclei of the $2s-2d$ shell, one can no longer speak of a quasimolecular structure. However, in these nuclei too there are analogous features in the energies of the holes and particles, which leads to an energy gap between transitions from different shells and weak mixing of these particle–hole states. Formally, this is due to the circumstance that when the quantum numbers n and l of the nucleons increase the Majorana forces rapidly lose their supermultiplet action, and the effect of the exchange operator P^x_{ij} becomes slight. In such a situation, the transitions $1p \to (2s-2d)$ and $(2s-2d) \to (3p-3f)$ are not on an equal footing.

Configuration splitting in nuclei of the $2s-2d$ shell is also realized in the Hartree–Fock method.[47] In this case, the part played by the Majorana forces is manifested as an increase in the deformation of the nucleus (as occurs in the nuclei ^{9}Be and ^{12}C), but the single-particle orbitals have a much more complicated form than the Nilsson orbits. As a result, the low-energy group of dipole transitions is associated with the excitation of valence nucleons, and the high-energy group with the excitation of nucleons of a closed shell.

With increasing atomic number A, when the values n and l of the valence shells increase, the exchange operator P^x_{ij} loses its importance (in nuclei of medium mass, the interaction range between the nucleons is already significantly less than the radius of the nucleus). The short-range nature of the interaction leads to the phenomenon of pairing. Qualitatively, a Cooper pair corresponds to the case when the residual interaction between the nucleons has the nature of δ-functional forces. In the relative motion, the Cooper pair of nucleons has the quantum numbers $N=2n$ and $L=0$, where n is the principal quantum number of the nucleons. Therefore, the wave function $\Psi_{NL}(r_{12})$ of the relative motion of such a pair has the maximal possible value[48] at $r_{12}=0$. This determines the nature of the coherent mixing of the various pairing states $(nlj)^2$ in a given oscillator shell, in which $n=\text{const}$. Basically, this is an entirely different effect from the long-range fouring effect discussed above; the $\tau\tau$ component of this δ-function interaction is attractive in the particle–particle channel and repulsive in the particle–hole channel.[4,49] This interaction lifts the incomplete degeneracy of the particle–hole states and shifts the resulting dipole state, since its energy is doubled compared with the energy $E_0 \approx 7-8$ MeV of the zeroth approximation.

Returning to light nuclei, we can say that, as follows from the qualitative consideration and estimates in the diagonal approximation, configuration splitting must occur in nuclei of the $1p$ and $2s-2d$ shells, this leading to the existence of two fairly well isolated groups of transitions A and B associated with excitation of nucleons of the valence and inner shells, respectively. In addition, within each group there may also be an energy splitting.

We now discuss the relative excitation intensity of these two branches. In nuclei in which there are fewer nucleons in the valence shell than in the closed shell, as, for example, in the Li or Mg isotopes, transitions of group B will predominate [see the expressions (1) and (2)]. Therefore, in such nuclei the dipole resonance will be situated at high energies. As the valence shell is filled, the intensity of the transitions from it naturally increases, while that of transitions from the closed shell decreases, since the number of states to which the dipole transitions can take place is reduced. As a consequence, the photonuclear dipole resonance maximum situated at lower energies than in nuclei in which the valence shell is just beginning to fill.

Configuration splitting and decay of the dipole resonance. Simultaneously with the conjecturing of the configuration splitting in light nuclei, it was pointed out that, since the mixing between the different groups of states is weak, the decay of each then must take place to corresponding hole states of the $A-1$ daughter nucleus.[9,10,20] The nucleon-decay scheme can be represented in the simplified form

$$A \nearrow 0s^4 1p^{A-5}, \quad \pi=(-1)^{A-1}; \tag{3a}$$

$$A \searrow 0s^4 1p^{A-6}(2s \text{ or } 2d)^1, \quad \pi=(-1)^{A}; \tag{3b}$$

$$B \to 0s^3 1p^{A-4}, \quad \pi=(-1)^{A}, \tag{4}$$

for nuclei of the $1p$ shell, and the form

$$A \nearrow 0s^4 1p^{12}(2s-2d)^{A-17}, \quad \pi=+1; \tag{5a}$$

$$A \searrow 0s^4 1p^{12}(2s-2d)^{A-18}(3p \text{ or } 3f)^1, \quad \pi=-1; \tag{5b}$$

$$B \to 0s^4 1p^{11}(2s-2d)^{A-16}, \quad \pi=-1, \tag{6}$$

for nuclei of the $2s-2d$ shell.

Of course, the configurations (3b) and (4) or (5b) and (6) are mixed by the nucleon–nucleon interaction. However, in this case too the mixing is generally of a kind that permits the identification of a configuration which makes the main contribution to the wave function.

The dipole resonance decays mainly by the emission of nucleons. The lightest nuclei of the $1p$ shell are an exception. The decay of group A through the nucleon channel must lead to the population of low-lying states of the final nucleus, whose structure is determined by the configurations $0s^4 1p^{A-5}$ (for nuclei of $1p$ shell) and $0s^4 1p^{12}(2s-2d)^{A-17}$ (for nuclei of the $2s-2d$ shell). In the first case, nucleons with orbital angular momenta $l=0$ and 2 will be emitted; in the second, nucleons with $l=1$ and 3. The decays indicated by the broken arrows, $3d$ and $5d$, will proceed much less strongly, since the energy and spectroscopic factors are in this case un-

favorable.

In the absence of mixing between groups A and B, the latter leads through decay to the population of only those states of the $A-1$ nucleus in which there is a hole in the closed 0*s* shell (in 1*p*-shell nuclei) or 1*p* shell (in nuclei of the 2*s*–2*d* shell). These hole states of the $A-1$ nucleus have a high energy (see the discussion below). Although the actual resonance due to the transitions of the group B is also situated fairly high, its decay, being associated with high hole states of the final $A-1$ nucleus, must lead to the emission of soft nucleons. In nuclei of the 1*p* shell, the decay of states of the group B will lead to the emission of a nucleon with $l=1$, and the decay of nuclei of the 2*s*–2*d* shell to the emission of nucleons with $l=0$ and 2.

The low-lying states of the final nucleus $A-1$ with parity $\pi=(-1)^A$ in nuclei of the 1*p* shell and $\pi=-1$ in nuclei of the 2*s*–2*d* shell contain predominantly the components (3b) or (5b), respectively, and a small admixture of the components (4) or (6). In Table II, we give the weights[50] of the 0*s* hole configuration in the wave functions of the nucleus ^{15}N with quantum numbers $J^\pi=\frac{1}{2}^+$. With increasing excitation energy the weight of the deep hole component in each state increases. Because of the presence of such admixtures in the wave functions of the final nucleus, a transition arises from the high-lying states of the giant resonance with deep hole to the low-lying states of the final nucleus through the deep hole component, which results in an additional relatively hard component in the photonucleon spectrum. In nuclei of the 2*s*–2*d* shell, this component has an appreciable intensity.

Knowledge of the hole nature of the populated states of the $A-1$ nucleus and the energy dependence of the partial cross sections makes it possible to decompose the giant dipole resonance into components associated with transitions of nucleons from different shells. For this, it is necessary to obtain separately the sums of the partial cross sections corresponding to formation of the final nucleus $A-1$ in hole states in the outer and the inner shell.

Thus, the decay of each group of states leads to the population of levels of the final nucleus $A-1$ which differ in their structure, energy, and parity, while the emitted nucleons differ in their orbital angular momenta. This specific nature of the decay of the groups A and B predetermined the ways in which they are identified experimentally. These are based on

TABLE II. Distribution of the 0*s* hole component over the different states of the nucleus ^{15}N with the quantum numbers J^π, $T=\frac{1}{2}^+, \frac{1}{2}$.

Excitation energy, MeV	Fraction of 0*s* hole component, %	Excitation energy, MeV	Fraction of 0*s* hole component, %
5.3	1.1	22.8	0.6
9.3	0.1	24.0	0.7
12.1	0.7	26.2	5.0
13.9	0.1	27.8	1.4
16.2	0	30.3	0.6
17.9	0	31.5	0.6
19.4	0	34.8	59.7
21.9	0.1	36.0	9.4

study of the so-called *partial cross sections*, i.e., the cross sections of reactions with the formation of the final nucleus in a definite state.

Important information is also contained in a characteristic of the partial cross section such as the angular distribution. Analysis of this characteristic makes it possible to extract the angular momentum of the emitted nucleon, which depends on the group of states that decays.

In nuclei in which the 1*p* shell is only beginning to be filled, the states of the final nucleus containing a hole in the 0*s* shell are unstable against subsequent complete breakup into fragments. In this group, the most probable decay channel is that of breakup into several particles, the so-called *star decay*. The precise nature of the fragments is determined by the Young tableau of the final state. A qualitative analysis of this kind was the basis of the first prediction[9,10] of the star decay of states formed by transitions of group B in the nuclei ^{6}Li and ^{7}Li and associated with quasi-α-particle absorption of photons:

$$0s^31p^3\,[321]\to\begin{cases}{}^3\mathrm{He}+d+n\\ {}^3\mathrm{H}+d+p\end{cases}\text{ and }0s^31p^4\,[331]\to\begin{cases}{}^3\mathrm{He}+n+{}^3\mathrm{H};\\ {}^3\mathrm{H}+p+{}^3\mathrm{H}.\end{cases}\qquad(7)$$

Of particular interest are the dipole states with the Young tableau [33] in ^{6}Li and [43] in ^{7}Li; the theory predicted[9,10] that they would decay predominantly through the ^{3}He–^{3}H and ^{4}He–^{3}H channels, respectively.

Possible experiments to detect configuration splitting of photonuclear dipole resonances. The partial cross sections can be extracted from the spectra of γ rays which de-excite the final nucleus and from the photonucleon spectra. At the present time, both types of experiment are made using a bremsstrahlung beam. As an example, Fig. 1 shows the spectra of γ rays emitted by the final nuclei produced by the decay of the dipole resonance in the nucleus ^{32}S. The spectra clearly reveal peaks corresponding to population as a result of the ^{32}S$(\gamma,p)^{31}$P reaction of nine levels of the nucleus ^{31}P in the region 3–6 MeV, and also a peak corresponding to population of the second excited state of the nucleus ^{28}Si as a result of the ^{32}S$(\gamma,\alpha)^{28}$Si reaction. The advantages of experiments if this type are: 1) the high-energy resolution of the Ge(Li) detector, which makes it possible to observe individual, even closely spaced, levels; 2) the possibility of obtaining in one experiment information about all the decay channels of the giant resonance—proton, neutron, α-particle, etc. The difficulties of the method are associated with the need to take into account correctly the cascade γ transitions, which complicate the picture of the population of the levels of the final nucleus, and the low photon detection efficiency of the Ge(Li) detector, which limits one to measurements at individual values of the upper limit of the bremsstrahlung and means that only integrated cross sections of transitions to the various states can be obtained (it is only in rare cases that one can obtain a rough energy dependence of the partial cross section). In addition, from the γ-ray spectra it is impossible to extract information about transitions to the ground state of the final nucleus and to states above the threshold of nucleon emission.

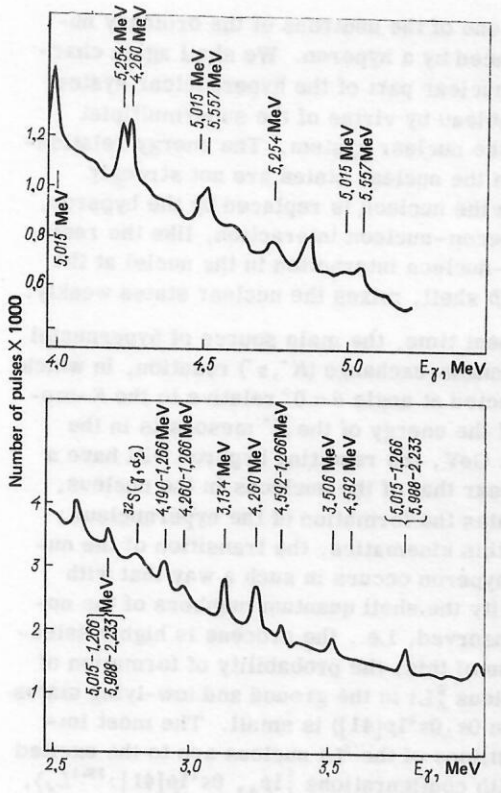

FIG. 1. Spectra of the γ rays emitted by the final nuclei produced by the decay of the giant dipole resonance of the nucleus ^{32}S.[51] Bremsstrahlung with the upper limit 27.3 MeV was used. The nature of the majority of the γ transitions is indicated.

In Fig. 2, for the example of the nucleus ^{32}S, we show typical photoproton spectra $N_p(E_p, E_\gamma^{max})$ for different values of the upper limit E_γ^{max} of the bremsstrahlung.[21] Each such spectrum is produced by the decays of many states of the giant dipole resonance to different levels of the final nucleus. If the photoproton spectra are measured for a set of bremsstrahlung spectra with

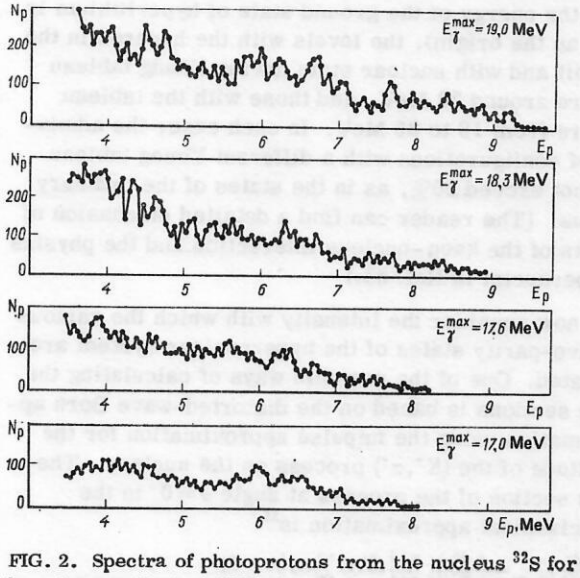

FIG. 2. Spectra of photoprotons from the nucleus ^{32}S for different upper limits E^{max} of the bremsstrahlung (E_γ^{max} = 17–19 MeV).[21]

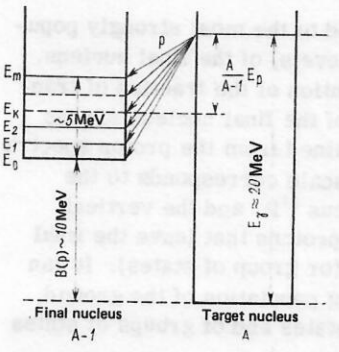

FIG. 3. Formation of the final nucleus through various states as a result of proton emission.

nearly equal upper limits, the transitions to different states of the final nucleus can be separated. The problem reduces to the solution of the system of linear equations

$$N_p(E_p, E_\gamma^{max}) = \sum_{k=0}^{m} \sigma_k(E_\gamma) W(E_\gamma, E_\gamma^{max}), \quad (8)$$

where $\sigma_k(E_\gamma)$ is the cross section of the partial photoproton reaction with formation of the final nucleus in state k ($k = 0, 1, 2, \ldots, m$), and $W(E_\gamma, E_\gamma^{max})$ is the bremsstrahlung spectrum. The proton energy E_p is related to the photon energy E_γ and the energy E_k of the final nucleus by (Fig. 3):

$$E_\gamma = B(p) + E_k + [A/(A-1)]E_p, \quad (9)$$

where $B(p)$ is the energy of proton separation.

The system of equations (8) can be solved for a restricted number of states of the final nucleus separated by a distance which does not exceed the step in E_γ^{max}. The partial cross sections $\sigma_k(E_\gamma)$ can be determined only for the states of the final nucleus that are most strongly populated in the (γ, p) reaction. To find such states from the proton spectra by means of the procedure described in detail in Refs. 24 and 52, one can obtain the distribution of the fraction of transitions to different states of the final nucleus. The maxima in

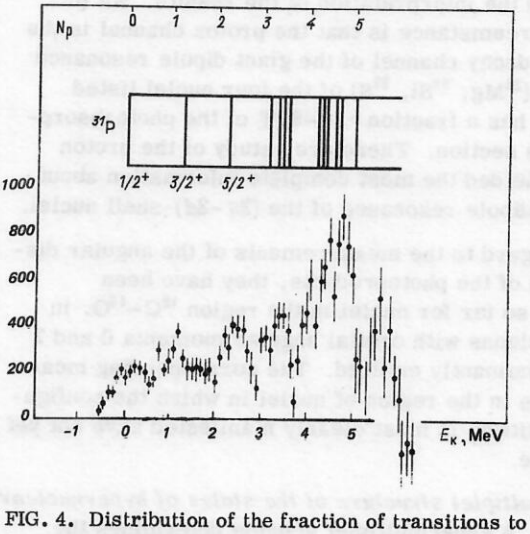

FIG. 4. Distribution of the fraction of transitions to the different states of the final nucleus for the reaction $^{32}S(\gamma, p)^{31}P$ obtained from the proton spectra shown in Fig. 2. The scheme of the lower levels of the nucleus ^{31}P is shown.

this distribution correspond to the most strongly populated levels (or groups of levels) of the final nucleus. Figure 4 shows the distribution of the fraction of transitions to different states of the final nucleus for the $^{32}S(\gamma,p)^{31}P$ reaction as obtained from the proton spectra in Fig. 2. The horizontal scale corresponds to the energy E_k of the final nucleus ^{31}P, and the vertical scale gives the number of protons that leave the final nucleus in a definite state (or group of states). It can be seen that there is strong population of the ground, first, and second excited states and of groups of states at higher energies.

The main advantage of the method of extracting the partial cross sections from the photonucleon spectra is the possibility of obtaining the detailed energy dependence of the partial cross sections, which is decisive in the study of configuration splitting. When the cross section for a group of unresolved states has been obtained from the photonucleon spectra, information indicating which of these states are populated can be given by an experiment which measures the spectra of the γ rays which de-excite the final nuclei. Thus, the most complete information about the partial cross sections is obtained in a combined investigation of the γ-ray and photonucleon spectra.

Such a program of investigations was realized for nuclei of the $2s-2d$ shell at the Scientific-Research Institute of Nuclear Physics at Moscow State University, where the photoproton spectra were measured and the partial cross sections were obtained for the proton decay channel of the giant dipole resonance by the method described above.[21-24] The analysis of these results used data on the γ-ray spectra obtained by other experimental groups. The nuclei ^{24}Mg, ^{26}Mg, ^{28}Si, and ^{32}S, for which the experimental material is the most extensive, were studied. At the same time, extensive spectroscopic information about the quantum numbers of the low-lying states of the final nuclei produced in the photoproton reaction (^{23}Na, ^{25}Na, ^{27}Al, ^{31}P) was obtained from proton pickup reactions, which facilitated the interpretation of the results. An important circumstance is that the proton channel is the dominant decay channel of the giant dipole resonance for three (^{24}Mg, ^{28}Si, ^{32}S) of the four nuclei listed above. It has a fraction ~70–80% of the photoabsorption cross section. Therefore, study of the proton channel yielded the most complete information about the giant dipole resonance of the $(2s-2d)$-shell nuclei.

With regard to the measurements of the angular distributions of the photoproducts, they have been made[53,54] so far for nuclei in the region $^{12}C-^{16}O$, in which nucleons with orbital angular momenta 0 and 2 are predominantly emitted. The corresponding measurements in the region of nuclei in which the configuration splitting is most clearly manifested have not yet been made.

Supermultiplet structure of the states of hypernuclear systems. A supermultiplet scheme determines the structure of not only ordinary nuclei at the start of the $1p$ shell but also, as was shown in Ref. 36, in Λ and, possibly, Σ hypernuclei. A hypernuclear system is formed when one of the neutrons of the ordinary nucleus is replaced by a hyperon. We shall again characterize the nuclear part of the hypernuclear system by a Young tableau by virtue of the supermultiplet structure of the nuclear system. The energy relationships between the nuclear states are not strongly changed when the nucleon is replaced by the hyperon, since the hyperon–nucleon interaction, like the residual nucleon–nucleon interaction in the nuclei at the start of the $1p$ shell, mixes the nuclear states weakly.

At the present time, the main source of hypernuclei is the strangeness-exchange (K^-,π^-) reaction, in which the π^- is detected at angle $\theta=0^\circ$ relative to the K-meson beam. If the energy of the K^- mesons is in the range up to 1 GeV, the resulting hyperon will have a momentum near that of the nucleons in the nucleus, which facilitates the formation of the hypernucleus. By virtue of this kinematics, the transition of the nucleon into a hyperon occurs in such a way that with high probability the shell quantum numbers of the nucleon are conserved, i.e., the process is highly selective. Because of this, the probability of formation of the hypernucleus $^6_\Lambda Li$ in the ground and low-lying states (configuration $0s_\Lambda 0s^4 1p[41]$) is small. The most important transitions of the ^6Li nucleus are to the excited $^6_\Lambda Li$ states with configurations $|1p_\Lambda, 0s^4 1p[41]:{}^{2S+1}L_J\rangle$, $|0s_\Lambda, 1\hbar\omega[41]:{}^{2S+1}L_J\rangle$, and $|0s_\Lambda, 1\hbar\omega[32]:{}^{2S+1}L_J\rangle$. Here, the symbol $1\hbar\omega[\lambda]$ means a state of the configuration $s^3p^2[\lambda]$. For $[\lambda]=[41]$, elimination of the center-of-mass motion is understood, so that in reality we are dealing with a superposition of the states $s^3p^2[41]$ and $s^4(2s-2d)[41]$.

In these transitions, the quantum number $J^\pi=1^+$ of the nucleus ^6Li is conserved. Calculation with allowance for the residual nucleon–nucleon and hyperon–nucleon interaction for hypernuclear states with total angular momentum $J^\pi=1^+$ confirms the supermultiplet nature of the hyperlithium levels and leads to the following structure of the levels: The levels with the hyperon in the $1p$ orbit are in the energy range 8–13 MeV (the energy of the ground state of hyperlithium is taken as the origin), the levels with the hyperon in the $0s$ orbit and with nuclear state having Young tableau [41] are around 20 MeV, and those with the tableau [32] are from 18 to 26 MeV. In each case, the admixture of configurations with a different Young tableau does not exceed 20%, as in the states of the ordinary nucleus. (The reader can find a detailed discussion of aspects of the kaon–nucleus interaction and the physics of hypernuclei in Ref. 55.)

We now consider the intensity with which the various positive-parity states of the hypernuclear system are populated. One of the possible ways of calculating the cross sections is based on the distorted-wave Born approximation using the impulse approximation for the amplitude of the (K^-,π^-) process on the nucleus. The cross section of the process at angle $\theta=0^\circ$ in the quasiclassical approximation is[55]

$$\left(\frac{d\sigma}{d\Omega}\right)_{\theta=0^\circ}=\left(\frac{d\sigma}{d\Omega}\right)_0\sum\left|\langle{}^6_\Lambda\mathrm{Li}|\sum_j u_j(n\to\Lambda)\times\exp\left\{iqz-\frac{\sigma}{2}T(b)\right\}|{}^6\mathrm{Li}\rangle\right|^2, \quad (10)$$

TABLE III. Energies and excitation cross section of the strongest resonances with spin 1^+ in hyperlithium formed in the (K^-, π^-) reaction with indication of the dominant configuration [the difference $\varepsilon(1p)-\varepsilon(0s)$ between the single-particle hyperon energies was taken equal to 7.5 MeV].

Excitation energy, MeV	$(d\sigma/d\Omega)_{\theta=0^\circ}$, μb/sr	Basic configuration of the resonance
8.4	1360	$1p_\Lambda$, $0s^41p$ [41] Group A
13.0	150	
18.0	840	$0s_\Lambda$, $0s^31p^2$ [32] Group B
19.7	185	$0s_\Lambda$, $0s^41d$ [41]
22.4	110	Superposition of various configurations
24.8	175	$0s_\Lambda$, $0s^31p^2$ [32]
26.4	180	$0s_\Lambda$, $0s^31p^2$ [32]
35.6	190	$0s_\Lambda$, $0s^31p^2$ [311]

where

$$T(b)=\int_{-\infty}^{\infty}\rho(b, z')\,dz'; \qquad (11)$$

ρ is the density of the nucleon distribution in the nucleus, and σ is the parameter of the pion–nucleon interaction. The resulting cross section for the production of the ${}^6_\Lambda$Li system in different states with total angular momentum $J^\pi=1^+$ is given in Table III, in which the principal component of the state wave function is indicated.

The resulting picture of the excitation is very similar to the case of the photonuclear reaction. At low energies, the transitions which form group A and are associated with the transition of a neutron from the outer shell to the hyperon in the $1p$ orbit are localized; there is then a gap around 5 MeV, after which the transitions that form group B are localized, a neutron of the $0s$ shell coming into play. Thus, one observes typical configuration splitting.

We now discuss the decay characteristics of hypernuclear resonances, which, as for ordinary nuclei, can be conveniently discussed in terms of spectroscopic factors. This was done for the first time in Ref. 36. The most strongly excited state at $E^*=8.4$ MeV, which is followed by one at 13 MeV, will, as is readily seen from the configuration which describes it, have the largest spectroscopic factor for emission of a $1p$ nucleon or $1p$ hyperon. The resonance next in intensity is at 18 MeV. Energetically, the decay of this resonance is allowed only through the channels ${}^5_\Lambda$He $+p$ and Li$+\Lambda$, where both ^{5}Li and ${}^5_\Lambda$He are in the ground state (Fig. 5). The dominant configuration (see Table III) is such that the decay to the ground state of both ${}^5_\Lambda$He and ^{5}Li is forbidden for this component and proceeds exclusively through the small admixture that disturbs the supermultiplet structure. As a result, the decay width for this resonance is much less than for the preceding low-lying resonances. This difference in the width has the consequence that the maximal value of the cross section is associated with this level rather than with the lower level, whose excitation cross section is maximal. This conclusion of the theory is confirmed experimentally, as is clearly seen in Fig. 5.

The main decay channel of the state with energy 26.4 MeV is the channel $d+{}^4_\Lambda$He (or ${}^4_\Lambda$He* with subsequent emission of a γ ray and transition to the ${}^4_\Lambda$He ground state). This decay almost completely determines the width of this level and partly that of the level with energy 24.8 MeV. These predictions about the nature of the decay of the resonances in the hypernuclear system ${}^6_\Lambda$Li call for coincidence measurements of the products of the (K^-, π^-) reaction, namely, π^- meson and deuteron, π^- meson and proton, and possibly also π^- meson, deuteron, and γ ray. Such data will undoubtedly lead to a deeper understanding of the supermultiplet structure in the Li hypernucleus. A supermultiplet level scheme is also realized in the ${}^7_\Lambda$Li and ${}^9_\Lambda$Be systems. And, as a consequence of such a scheme, there will be specific channels of decay into two and three fragments, as in photodisintegration.

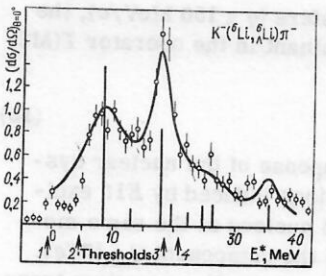

FIG. 5. Differential cross section at the angle $\theta=0^\circ$ of the reaction ${}^6\text{Li}(K^-, \pi^-)$ with allowance (continuous curve) and without allowance (vertical lines) for the width of the resonance.[36] The experimental data are taken from Ref. 56. The arrows indicate the thresholds for the decay of ^{6}Li through the following channels: 1) ${}^5_\Lambda\text{He}+p$, 2) ${}^5\text{Li}+\Lambda$, 3) ${}^4_\Lambda\text{He}+d$, 4) ${}^3\text{He}+{}^3_\Lambda\text{H}$.

Configuration splitting of a dipole resonance excited by electron scattering, μ capture, and radiative capture of π mesons. Hitherto, we have mainly discussed photonuclear dipole resonance. There are two further families of electromagnetic transitions of the dipole type, but only with respect to the orbital part of the operator. One of the families is formed by magnetic quadrupole transitions ($M2$), and the second by transverse electric dipole transitions ($E1t$), which arise in the case of backward electron scattering. The corresponding operators are

$$T(M2;\, q)=\mathrm{i}\frac{q}{2M}\Big\{-Q_{122}(\nabla/q)+\frac{\mu_p+\mu_n}{2}\Big[\sqrt{\tfrac{3}{5}}Q_{112}(\sigma)-\sqrt{\tfrac{2}{5}}Q_{132}(\sigma)\Big]-Q_{122}(\nabla/q)\tau_3+\frac{\mu_p-\mu_n}{2}\tau_3\Big[\sqrt{\tfrac{3}{5}}Q_{112}(\sigma)-\sqrt{\tfrac{2}{5}}Q_{132}(\sigma)\Big]\Big\}; \qquad (12)$$

$$T(E1t;\, q)=\frac{q}{2M}\Big\{\Big[\sqrt{\tfrac{2}{3}}Q_{101}(\nabla/q)-\sqrt{\tfrac{1}{3}}Q_{121}(\nabla/q)\Big]+\frac{\mu_p+\mu_n}{2}Q_{111}(\sigma)+\tau_3\Big[\sqrt{\tfrac{2}{3}}Q_{101}(\nabla/q)-\sqrt{\tfrac{1}{3}}Q_{121}(\nabla/q)\Big]+\frac{\mu_p-\mu_n}{2}\tau_3 Q_{111}(\sigma)\Big\}, \qquad (13)$$

where

$$Q_{1wI}(\mathbf{a})=j_w(qr)\,[Y_w(\mathbf{r})\otimes\mathbf{a}]_{IM}; \qquad (14)$$

q is the momentum transfer; μ_p and μ_n are the magnetic moments of the proton and neutron in nuclear magnetons.

At small momentum transfers ($q \lesssim 150$ MeV/c), the isovector component is dominant in the operator $T(M2; q)$:

$$(\mu_p - \mu_n)\,\tau_3 Q_{112}\,(\sigma)/2, \tag{15}$$

and this determines the response of the nuclear system. For isoscalar transitions induced by $E1t$ excitations, the response of the nucleus at the same momentum transfers is due to the component $Q_{101}(\nabla/q)$. In isovector excitations at very small momentum transfers the component $\tau_3 Q_{101}(\nabla/q)$ is dominant. The spin component of the operator plays a small part at such small momentum transfers but it increases in importance with increasing momentum transfer. A short list[57] of single-particle matrix elements of the isovector component of the operators $T(M2)$ and $T(E1t)$, calculated using harmonic-oscillator wave functions, illustrates what we have said for the example of $1p \to 2s$ and $2d$ transitions (Table IV).

Like the photonuclear resonances, the resonances associated with the $E1t$ and $M2$ excitations are formed mainly by transitions of nucleons to a neighboring shell, though at the same time there is also a reversal of either the spin ($M2$ transition) or the orbital angular momentum ($E1t$ transition).

Giant resonances are also excited when muons are absorbed. They arise predominantly from first-forbidden transitions (using the terminology of the theory of β decay, which is also employed in the theory of μ capture); the only exceptions are heavy nuclei (for more details, see Ref. 26). Since the weak interaction is due to vector and axial-vector currents, first-forbidden transitions correspond to excitations of both dipole type, which are isobaranalogs of the photonuclear dipole resonance, and spin–dipole type. The angular part of the operator of the spin–dipole transition has the form

$$\hat{O} = [Y_1 \otimes \sigma]_{J=0^-,\,1^-,\,2^-} \tag{16}$$

and completely agrees with (15) and, ultimately, with (12) for $J=2$.

In the radiative capture of stopped π mesons ($\pi^- A \to A^* \gamma$) by $1p$-shell nuclei, the main contribution to the process is also due to spin–dipole transitions.[26] The spin–angle part of the transition operator is identical to (16).

TABLE IV. Single-particle matrix elements of the isovector component of the operators $T(E1t, q)$ and $T(M2, q)$.

$n_i l_i j_i - n_f l_f j_f$		$T(E1t, q)$		$T(M2, q)$	
	$n_i l_i j_i$	$1p_{3/2}$	$1p_{1/2}$	$1p_{3/2}$	$1p_{1/2}$
$2d_{5/2}$	a	−0.0677	—	0.0032	−0.0028
	b	−0.0045	—	0.0625	−0.0549
$2s_{1/2}$	a	−0.0346	−0.0221	0.0019	—
	b	−0.0524	0.0340	0.0335	—
$2d_{3/2}$	a	0.0265	−0.0540	0.0009	−0.0003
	b	0.0788	−0.0725	0.0203	−0.0028

Note. a) $q = 20$ MeV/c, b) $q = 100$ MeV/c.

We shall now illustrate the general features and differences in the nature of the interaction of these fields with nuclei. The $\Delta J = 2, \Delta T = 1$ transitions in the range of momentum transfers 50 MeV/$c \lesssim q \lesssim 150$ MeV/c in all three reactions are due to virtually the same operator (16), which differs only slightly from the $M2$-transition operator. Therefore, the gross structure of the excitation curve in the $\Delta J = 2$ transitions is the same for all the considered reactions. The $\Delta J = 1, \Delta T = 1$ transitions associated with absorption of muons are due to both the dipole and the spin–dipole operator; in radiative capture of π mesons, to only the spin–dipole operator; and in backward scattering of electrons, to the operator $T(E1t; q)$. Because of the different structures, the response of the nucleus will in this case depend on the particular perturbation.

Although all the considered transitions are of the dipole type with respect to the orbital part, they have a number of differences from the purely dipole transitions realized in photoabsorption. One of these is that for $M2$ transitions in the zeroth approximation a group of quasidegenerate levels is not formed even in nuclei with closed shells. The dipole resonance is determined basically by $(l + \frac{1}{2}) \to (l + 1 + \frac{1}{2})$ transitions and to a lesser extent by $(l - \frac{1}{2}) \to (l + 1 - \frac{1}{2})$ transitions without spin flip, and therefore the spin–orbit splitting does not come into play and does not broaden the absorption band in the zeroth approximation. As can be seen from Table IV, the $M2$ excitations lead to large amplitudes of the transitions $(l + \frac{1}{2}) \to (l + 1 + \frac{1}{2})$ and with spin flip $(l - \frac{1}{2}) \to (l + 1 + \frac{1}{2})$ and to a lesser degree $(l + \frac{1}{2}) \to (l + 1 - \frac{1}{2})$. The first two are separated from each other in the zeroth approximation by about the energy of the spin–orbit splitting, and the last two by about twice this energy, which in medium and heavy nuclei is about 10 MeV. Therefore, $M2$ resonance must be characterized by strong configuration splitting within a given group of transitions even for nuclei with closed shells, but its physical nature is quite different from that of the dipole resonance in light nuclei—it is due to the spin–orbit splitting. But the splitting between the groups A and B has the same origin as before. Thus, even in medium and heavy nuclei the $M2$ resonance is not so collectivized as the photonuclear dipole resonance, since the residual nucleon–nucleon interaction is incapable of collecting such widely separated groups of transitions into a single maximum.

These factors may ultimately have the consequence that the $M2$ transitions are spread over a broad energy range. An additional spread is due to the influence of states of more complicated nature (of the type $2p$–$2h$, etc.). It can then happen that even in medium nuclei there is no appreciable concentration of the strength of the $M2$ transitions. The experimental situation is apparently close to this.

The transverse $E1$ excitations differ from the dipole excitations in the following respect. For $1p$-shell nuclei, the most intense transitions are $1p \to 2d_{3/2}$ and $0s \to 1p_{1/2}$. Because of this, the entire resonance is shifted to higher energies, the groups A and B approach each other, and the intensity of the latter does

not decrease significantly as the shell is filled. However, this interesting effect is most clearly manifested in nuclei of the $2s-2d$ shell, for which the most intense group $1p_{3/2} \to 2d_{3/2}$ of transitions lies approximately 5 MeV higher than the group B of the giant dipole resonance $1p_{3/2} \to 2d_{5/2}$, and it takes up a greater fraction of the sum rule. The active part played by the spin–orbit splitting is here manifested again. The same group of transitions is also revealed as the most intense in μ capture. Experimentally, all these equations have as yet been little studied. But we believe that such considerations will stimulate the necessary experiments. We shall return to a more detailed discussion of these questions in the following section.

Fragmentation of deep hole states of light nuclei. To describe the states that form a dipole resonance, and also the states of the final nucleus to which the decay takes place, it is necessary to know the positions of not only the single-particle but also the hole states of the average field. The corresponding quantities are parameters of the theory, and they are obtained on the basis of the best description of the experimental spectrum of a large number of nuclei by fitting through variation (in medium and heavy nuclei, one can choose a potential of the average field which gives all these quantites simultaneously). Thus, if we restrict ourselves to dipole transitions within the $1\hbar\omega$ excitation band, then, as follows from (1), to calculate $1p$-shell nuclei we need information about the positions of the single-particle $2s_{1/2}, 2d_{5/2}, 2d_{3/2}, 1p_{3/2}$, $1p_{1/2}$ states and the $0s$ hole state. The values for the first three are chosen on the basis of the experimental data on the lowest positive-parity levels of nuclei with the atomic numbers $A = 13$ and 17 and so forth. The last two can be selected either on the basis of the experimental data on the level spectrum of nuclei with $A = 5$, or, with better justification, on the basis of the best agreement in the description of the low-lying states of all nuclei of the $1p$ shell (this last procedure is realized in Ref. 58). In nuclei of the $2s-2d$ shell, as follows from (2), we require information about the single-particle $2s_{1/2}$, $2d_{3/2}$, $3p$, and $3f$ states and the $1p_{3/2}$, $1p_{1/2}$, and $2d_{5/2}$ hole states.[2)]

Information about the hole states is obtained from the experimental data on quasielastic proton knockout $(p,2p)$ or $(e,e'p)$ or the pickup reactions (p,d), $(d,{}^3\mathrm{He})$, $(t,{}^3\mathrm{He})$, $(t,{}^4\mathrm{He})$, etc. In these experiments, one measures the fragmentation of the hole state over the excitation spectrum (over the hole levels) of the produced $A-1$ nucleus, it being borne in mind that the distribution of the excitation probabilities of the hole levels is different in the different processes. On the basis of such experimental data, the positions of the hole states are then determined.

In quasielastic knockout reactions, we find the energy of proton separation for shells with different quantum numbers nlj and proton number $\langle p\rangle_{nlj}$ in these shells. Thus, these reactions make it possible to obtain the positions of the proton hole levels in the nuclei. The $(p,2p)$ and $(e,e'p)$ reactions are particularly convenient for studying the positions of the deep hole states ($0s_{1/2}^{-1}$ in $1p$-shell nuclei and $1p_{3/2}^{-1}$ in nuclei of the $2s-2d$ shell), since in these reactions a broad region of excitation energies in the final nucleus (up to 80–100 MeV) is investigated, and the absorption in the exit channel is here comparatively weak. Because of the low energy resolution (1.5–2.0 MeV), the quasielastic knockout reactions give averaged information about the quantum numbers of the groups of states in the final nucleus. As a result, one can determine only the centers of gravity of the hole states belonging to different shells and the region over which they are spread.

The results of Refs. 59–61 on quasielastic knockout are systemized in Fig. 6, which reflects the behavior of the proton separation energy with increasing atomic number of the nucleus. It is important that the deep hole states ($0s^{-1}$ and $1p^{-1}$) are spread over a broad range of excitation energies (~20 MeV), and some of the $1p^{-1}$ states of the nuclei of the $2s-2d$ shell are at an excitation energy below 10 MeV. This is an important result, from which it follows that already the low-lying states with the configuration (5b) contain a small admixture of configurations of the type (6), and the possibility of states of the group B decaying to them is opened up. The corresponding experimental data will be given in a review devoted to nuclei of the $2s-2d$ shell, in which the intensities with which the states of the final nucleus are populated in photodisintegration and pickup reactions are compared.

In proton pickup reactions [such as $(d,{}^3\mathrm{He})$ or $(t,{}^4\mathrm{He})$] there is also predominant excitation of proton hole states, and the high energy resolution (20–30 keV) makes it possible to investigate the individual states. For each state, one determines the orbital angular momentum l of the pickup proton and the spectroscopic factor S; the following sum rule must be satisfied:

$$\sum \frac{2T}{2T+1} S = \langle p\rangle_{nlj}, \qquad (17)$$

where T is the isospin of the final nucleus, and the summation is over all states of the final nucleus that can be reached as a result of proton pickup from the subshell with quantum numbers nlj. The accuracy of the determination of the spectroscopic factors in pickup reactions is about 25%.

An important outcome of such investigations is the obtaining of information about the distribution of the corresponding hole configuration over the states of the $A-1$ nucleus. However, because of the strong absorption, pickup reactions give information for only a restricted region of low excitation energies of the final nucleus (as a rule, not higher than 10 MeV). In this region, the observed states exhaust the sum rule for the hole excitations in the outer shell. In addition, in nuclei of the $2s-2d$ shell the observed $1p_{1/2}^{-1}$ states exhaust the sum rule for the $1p_{1/2}$ subshell. With regard to the deep hole states, in $1p$-shell nuclei the $0s^{-1}$ states are not seen at all in pickup reactions, since only a low excitation energy is accessible, and in nuclei of the $2s-2d$ shell the observed $1p_{3/2}^{-1}$ states ex-

[2)] If the point of departure is a closed $2d_{5/2}$ shell.

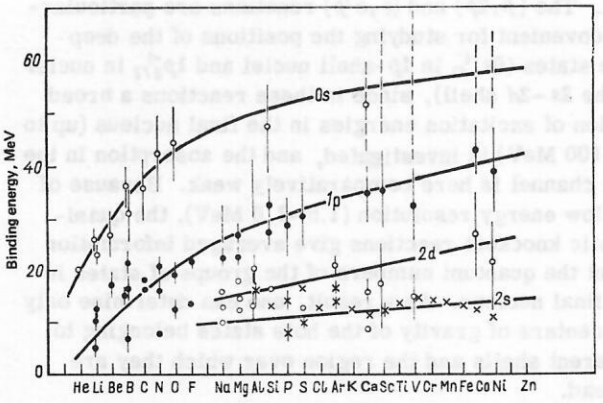

FIG. 6. Binding energies, widths, and orbital angular momenta for hole states obtained in the quasielastic knockout reactions $(p,2p)$ and $(e,e'p)$.[59,60]

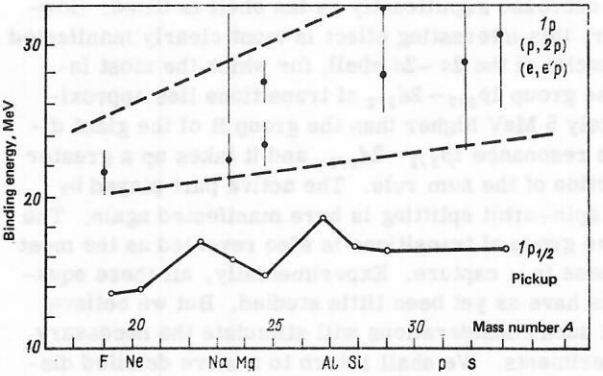

FIG. 7. Proton binding energy in the $1p$ shell from quasielastic knockout reactions (see Fig. 6) and in the $1p_{1/2}$ subshell from pickup reactions for nuclei of the $2s$–$2d$ shell.

haust on the average only about 40% of the sum rules for the $1p_{3/2}$ subshell. Thus, in pickup reactions for the $(2s-2d)$-shell nuclei we see only part of the spectroscopic strength of the $1p_{3/2}^{-1}$ state because of the energy limitation and, therefore, from pickup reactions we can extract information about the position of the center of gravity of only the $1p_{1/2}^{-1}$ states of the $(2s-2d)$-shell nuclei (Fig. 7).[62-72] For comparison, in Fig. 7 we also give data on the positions of the centers of gravity of the $1p^{-1}$ states obtained in quasielastic knockout reactions. The results of the experiments investigating the binding energies of a proton in an inner shell given in Fig. 7 can be explained using the factors discussed above—the strong spread over the energy of the $1p_{3/2}^{-1}$ states and the absence of a significant fraction of the spectroscopic strength of these states in the pickup reactions.

We now return to $1p$-shell nuclei and analyze the experimental data on the knockout of 0s nucleons. Outer-shell nucleons are analyzed in detail in Refs. 38 and 73.

Quasielastic knockout is usually analyzed in accordance with the following scheme. We write the differential cross section of quasielastic knockout in the form (see, for example, Ref. 59):

$$d\sigma/(dE_1 dE_2 d\Omega_1 d\Omega_2) = F\,(d\sigma/d\Omega)_0 S\,(\mathbf{p},\ E^*). \tag{18}$$

where F is a known kinematic factor, $(d\sigma/d\Omega)_0$ is the differential cross section for scattering on the free proton, and $S(\mathbf{p},E^*)$ is the structure factor, equal to

$$S\,(\mathbf{p},\ E^*) = \sum_{\alpha} |\,\Phi_\alpha\,(\mathbf{p})\,|^2\, S_\alpha\,(E^*). \tag{19}$$

where $|\Phi_\alpha(\mathbf{p})|^2$ characterizes the momentum distribution of the protons in the shell with quantum numbers $\alpha = |n,l,j\rangle$, $S_\alpha(E^*)$ is the spectral function, and E^* is the proton separation energy. In the general case, the spectral function is found by solving the differential equations[74] that describe the dynamics of the process. However, for practical purposes a simplified variant of the calculation has so far been used in which the nuclear form factor is obtained by means of harmonic-oscillator wave functions. The form factor is proportional to $\Phi_\alpha(\mathbf{p})$. A further simplification is associated with the use of plane waves for the incident and scattered wave.

The energy part of the spectral function, $S_\alpha(E)$, is usually taken[75] as a sum of Breit–Wigner resonances with constant width Γ_γ:

$$S_\alpha\,(E) = \sum_{\gamma=1}^{N} S_\alpha^\gamma \frac{\Gamma_\gamma^2/2}{\pi\,[\Gamma_\gamma^2/4 + (E-E_\alpha)^2]}. \tag{20}$$

The summation is over all states of the residual nucleus.

The factor S_α^γ for $1p$-shell nuclei can be calculated using shell-model wave functions[28,76,77] constructed with allowance for all nucleon transitions in the $1\hbar\omega$ excitation band with inclusion of the residual nucleon–nucleon interaction but the exclusion of the so-called spurious states corresponding to motion of the nucleus as a whole. The ground state of the initial nucleus is described in the shell model with intermediate coupling and parameters taken from Ref. 58. The remaining details of the calculation are not so important, and if necessary can be found in Ref. 77.

In Fig. 8, we give three examples of the description of the spread of the hole configuration; these illustrate the state of the relationship between the experiments and the particular variant of the theory. The width Γ_γ in (20) was varied from $\Gamma_\gamma = 1$ to 20 MeV. In the calculation, the energy of the 0s hole state was set equal to $\varepsilon(0s) = -20$ MeV, as follows from Fig. 6. The experimental data were taken from Ref. 78.

Despite various strongly simplifying assumptions, the theory gives the main features of the fragmentation of the 0s hole configurations. Important here is the use of a large basis for constructing the corresponding wave functions. The theory reproduces the center of gravity of the proton-knockout energy rather well. In the nuclei considered, it is 29 MeV (^{9}Be), 34.5 ± 1.5 MeV (^{12}C), and about 42 MeV (^{14}N) according to the measurements, while the calculation of Ref. 77 gives 31, 34, and 38 MeV, respectively.

The contribution of the 0s hole configuration can be followed to low excitation energies (see also Table II), though it decreases rapidly with decreasing energy. The experimentally observed tendency for the center of gravity of the hole state to be shifted to higher energies

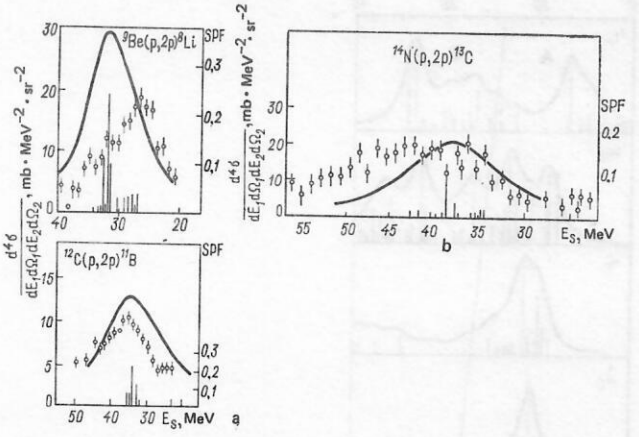

FIG. 8. Spectroscopic factors (vertical lines) (SPF), the spectral function $S_\alpha(E)$ (continuous curve), and the differential cross section for 0s-proton knockout in the $(p,2p)$ reaction[77]: a) $\Gamma_y(E^* \leq 30$ MeV) = 6 MeV, $\Gamma_y(E^* > 30$ MeV) = 8 MeV, b) $\Gamma_y = 18$ MeV, c) $\Gamma_y = 10$ MeV.

as the outer $1p$ shell is filled is manifested. Bearing in mind the approximations that had to be made in the derivation of (19) and (20), we can say that, overall, the theory describes the experimentally observed nature of the fragmentation of the hole 0s configuration.

To reproduce the localization region of the hole configuration, the values that were used for Γ_y were in the range 8–18 MeV. Naturally, the high-energy excitation region is depleted in the theory. It is probably due to admixture of high-lying shells, which are not encompassed by the calculation.

Summarizing our brief discussion of the fragmentation of the deep hole configurations of light nuclei, we note that the employed approach and the choice of the parameters have made it possible to reproduce the basic features of the effect. It is therefore natural to use the same procedure for constructing the wave functions in the part of the calculations of other processes that are associated with the fragmentation of deep hole states. Such a program was carried out in various papers, the results of which are reviewed in Ref. 79.

As we have already said, the nature of the excitation of the hole state depends strongly on the process actually under consideration; therefore, it is not always possible to match the data on the $(p,2p)$ reaction to photonuclear data. For example, in the $(p,2p)$ reaction on nuclei with spin zero only states of the $A-1$ nucleus with isospin $T=\frac{1}{2}$ are excited; this corresponds not to the ground-state $T=3/2$ but to the $T_<$ branch of the resonance in this nucleus. In nuclei with $T_i=\frac{1}{2}$, states of the final nucleus with isospin $T=1$ are excited in the $(p,2p)$ reaction, which corresponds to the ground-state branch of the resonance. In this way, photonuclear and other reactions can serve as additional sources of information about the fragmentation of deep hole configurations.

We draw attention to the important case of knockout of a 0s proton from ^{7}Li, which leads to the formation of ^{6}He with the configuration $0s^3 1p^3[33]^{33}P$. This last has already been encountered above in the discussion of the photodisintegration of ^{6}Li through the channel ^{3}He + ^{3}H. In this case, there is a close correlation between the two processes (see Sec. 2).

In $(2s-2d)$-shell nuclei, a theoretical analysis of the fragmentation of the hole states of this kind has not been made. All that is known are detailed calculations of the spectroscopic factors for the outer nucleons.[80] Such a situation arises because the number of states which must be included in the calculation is huge. In this connection, great importance attaches to experimental information that, without detailed calculations, makes it possible to judge the nature of the corresponding nuclear state, i.e., the information on quasielastic knockout and pickup reactions discussed above. It is here natural to rely on the experience acquired in the calculation of $1p$-shell nuclei.

Here, we shall not discuss the spread of the hole states in $(2s-2d)$-shell nuclei.

Basic features of configuration splitting of dipole resonances. We shall now summarize our consideration of configuration splitting of dipole and spin–dipole resonances in light nuclei. The phenomenon of configuration splitting reduces to the formation of two groups of transitions (A and B) that are separated in energy, overlap weakly, and are formed by nucleons from different shells. The transitions within each group can also be split into groups, the nature of which is determined by the supermultiplet structure of the levels. As a consequence of all this, there are specific features of the decay of each group of states that form a resonance. Group B decays predominantly into highly excited states of the final nucleus containing a hole in a closed shell. And although this branch of the resonance has a high position, its decay does not lead to the production of high-energy nucleons. In nuclei at the start of the $1p$ shell, star decay of the states of group B is predominant.

To establish these features, we have used a rather crude form of theory based essentially on the diagonal approximation. Naturally, the next step was to use a better variant of the theory, taking into account, first, the nondiagonal part of the residual nucleon–nucleon interaction and, second, not only the configurations directly coupled to the ground-state configurations of the nucleus through the dipole transitions but also the configurations that ensure the spreading of the resonance.

For many nuclei of the $1p$ shell, calculations were made[79] of the excitation of dipole resonances with allowance for all configurations corresponding to the transitions $0s \to 1p$ and $1p \to 2s$ or $2d$ with subsequent nucleon decay into a large number of states of the final nucleus. In such an approach, the theory gives a significantly better description of the experimental data as regards the localization region of the resonance and its gross structure. In nuclei of the $2s-2d$ shell, one must have recourse to various approximations to limit the number of states from which the dipole-resonance states are constructed, since the total number of them

is huge. It is usually assumed that the $2d_{5/2}$ shell is maximally filled. Thus, in the nucleus ^{32}S one proceeds from the configuration $0s^4 1p^{12} 2d_{5/2}^{12}(2s-2d_{3/2})^4$ for the ground state and $0s^4 1p^{11} 2d_{5/2}^{12}(2s-2d_{3/2})^5$, $0s^4 1p^{12} 2d_{5/2}^{11}(2s-2d_{3/2})^4$ ($3p$ or $3f$), and $0s^4 1p^{12} 2d_{5/2}^{12}(2s-2d_{3/2})^3$ ($3p$ or $3f$), respectively, for the states of the giant resonance. The problem is then a many-body problem only as regards the distribution of the four nucleons over the $2s-2d_{3/2}$ subshell. However, in such an approach the resonance is strongly concentrated on a few states, which is not so in reality. To spread the resonance, one includes phonon excitations, as is done, for example, in Ref. 25. Despite the great success of the theory in describing many features of dipole resonance, it must be borne in mind that in many important points the theoretical studies have not yet achieved quantitative success, this applying especially to the decay of the resonance into fragments.

In what follows, we shall discuss the results of these more complete calculations and the results of many years of experimental study, having in mind essentially configuration splitting.

2. REALIZATION OF CONFIGURATION SPLITTING OF DIPOLE RESONANCE IN 1p-SHELL NUCLEI (THEORY AND EXPERIMENT)

Total photodisintegration cross section. The calculated total photoabsorption cross sections[79,81] are given in Fig. 9, and the experimental cross sections[46,82-84] in Fig. 10. The vertical lines show the calculated integrated excitation cross sections of the strongest resonances. The curves are plotted under the assumption that each resonance has a Lorentzian profile and width equal to 2 MeV. The contributions of all resonances, including weak ones, were taken into account in the construction of the curves. For the nuclei ^{9}Be and ^{11}B, only the $T_>=3/2$ branch of the resonance was calculated. The experimental data also correspond to total absorption.

The integrated cross section of photoabsorption in ^{6}Li, found with allowance for the nondiagonal part of the nucleon–nucleon interaction on the basis of all configurations corresponding to the $1\hbar\omega$ excitation is shown separately in Figs. 11b and 11c. The first result was obtained in Ref. 28 under the assumption that the ^{6}Li ground state can be described by the many-particle shell model; the second,[40] with allowance for cluster structure. Both approaches lead to qualitatively the same structure of the excitation spectrum of the nucleus. Moreover, the result is close to the result obtained originally in the diagonal approximation,[10] in which it was also shown that the main branch of the resonance lies at high energies. Allowance for the cluster structure of the ^{6}Li ground state leads, basically, to a decrease in the excitation intensity of the various groups. With regard to the differences in the energy positions of the groups in Figs. 11b and 11c, particular attention should not be paid to them. They merely indicate that the result is rather sensitive to the choice of the parameters of the model.

The total cross section of absorption in ^{6}Li has not been measured. There are experimental data on the neutron channel[85] (see Fig. 11a):

$$(\gamma, Tn) = (\gamma, n) + (\gamma, pn) + (\gamma, 2n) + (\gamma, p2n) + \ldots$$

It does not exhaust the complete cross section, since it does not include the neutronless channels $(\gamma, pd)t$ and $(\gamma, {}^3\mathrm{He})t$. The cross section of the first of these channels, $(\gamma, pd)t$, is shown in Fig. 11d. The contribution of the second is not very large and is not shown in the figure (it will be discussed later). The sum of the two experimental curves must reflect the total absorption cross section.

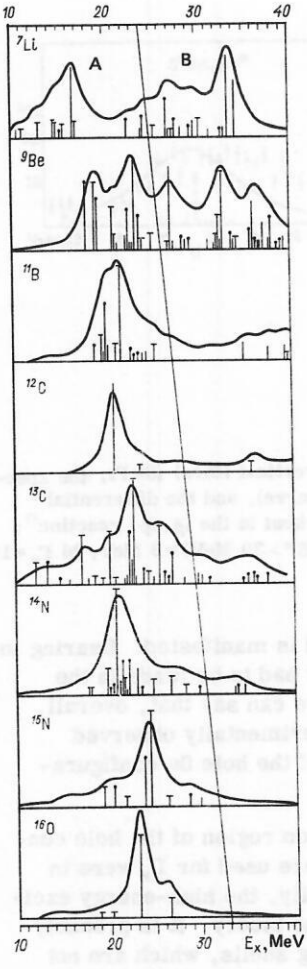

FIG. 9. Calculated[79,81] excitation spectrum of nuclei of the 1p shell in the case of photoabsorption.

1. An improved variant of the theory, which made it possible to take into account not only the nondiagonal part of the nucleon–nucleon interaction but also all the states (in the $1\hbar\omega$ excitation band) over which the resonance is distributed, completely confirmed all the predictions about configuration splitting drawn in Sec. 1 on the basis of the qualitative study. In Fig. 9, the transitions that lie to the right of the line which intersects the energy scale are due to nucleons of the deep 0s shell, i.e., the group B.

2. Whereas in the lithium isotopes the group B forms the greater part of the complete resonance, its contribution decreases as the 1p shell is filled, as can be clearly seen in Fig. 9, and in ^{11}B it is already small.

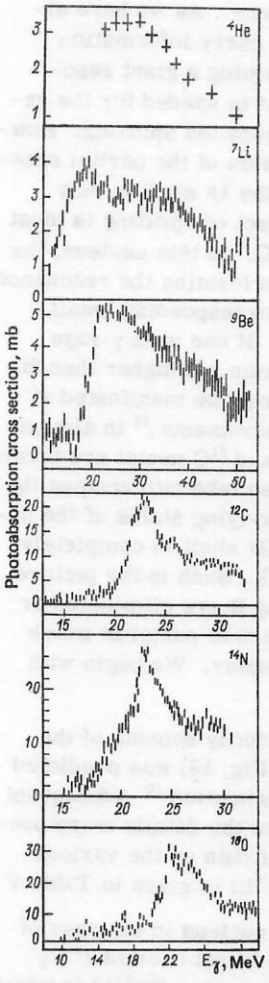

FIG. 10. Experimental cross sections of total photoabsorption in ^{4}He and nuclei of the $1p$ shell (Refs. 46 and 82–84).

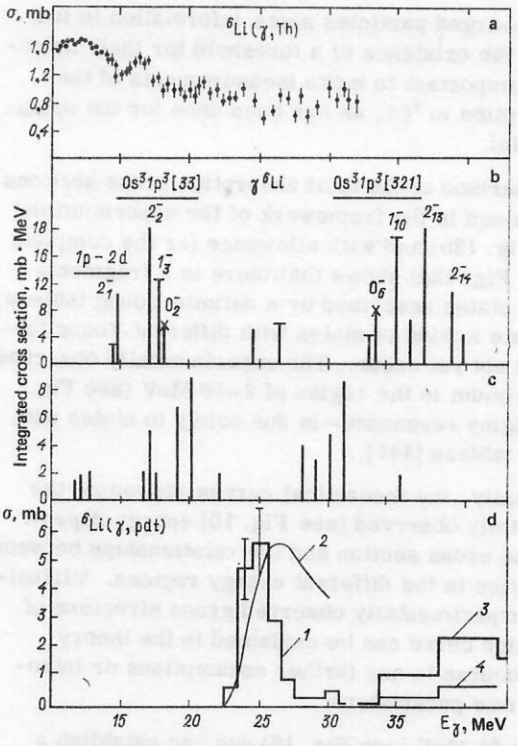

FIG. 11. Dependence of the neutron yield[85] in the reaction $\gamma + {}^6$Li (a), the total cross section of photoabsorption in ^{6}Li (Ref. 28) with allowance for all $1\hbar\omega$ excitations (b), the total cross section of photoabsorption in ^{6}Li (Ref. 40) with allowance for all $1\hbar\omega$ excitations and the $\alpha-d$ cluster structure in the ground state (c), and the (γ, pdt) reaction cross section[86] (the histogram 1) on the energy E_γ. The investigation of Ref. 87 revealed a high-energy maximum (histogram 3), some of which (histogram 4) decays through the pdt channel. Curve 2 is the result of calculation[88] in the framework of a simplified cluster model.

In the investigation of ^{12}C photodisintegration through various channels, (γ,n),[89] (γ,p),[90] (γ,pn),[90] and $(\gamma,p\alpha)$,[91] a small maximum was observed in the region of 35 MeV. The integrated cross section in the (γ,p) channel between 30 and 37 MeV is 17 mb · MeV.[90] It is in precisely this energy region that theory predicts localization of the transitions of group B.

In the ^{13}C(γ,n) reaction, an analogous maximum can be seen at 36 MeV,[92] and in the inverse ^{12}C$(p,\gamma)^{13}$N reaction at 33 MeV.[93] The theory predicts[9,94,95] the existence in this energy region of nucleon transitions from the $0s$ shell. Finally, in the ^{14}C$(p,\gamma)^{15}$N reaction a small peak is observed[96] at 37 MeV. According to the calculations of Refs. 97 and 98, the transitions of group B are localized in the same energy region.

Of course, it is only on the basis of this agreement between the theoretical and experimental values of the energy that one can say that these are transitions of the group B. For more definite conclusions, the available data are clearly inadequate. We need additional information on the partial cross sections for this excitation region and on the decay channels. It may be that this group of states undergoes star decay, as predicted in Refs. 9 and 12. This question will be discussed in the following section.

3. Once fouring at the nucleons has occurred in the $1p$ shell, the resonance branch (group A) corresponding to it is localized at a higher energy than in the preceding nuclei. Thus, as the $1p$ shell is filled there is, on the one hand, a tendency for the excitation energy to decrease because of the decreasing importance of transitions of the group B, but, on the other hand, this is matched by a tendency to an increase, since it is necessary to break up the nucleon quadruplet in the $1p$ shell. However, these two factors do not operate with equal strength, and at the end of the shell the center of gravity of the resonance is shifted to lower energies. As the $1p$ shell is filled, the transitions are concentrated in a fairly narrow energy region, although local maxima can still be seen in different parts of the spectrum.

4. Attention should be drawn to the similarity of the gross structure of the excitation spectra of the nuclei ^{7}Li and ^{9}Be. In the region from 20 to 40 MeV, the cross section changes slightly and there are no pronounced peaks in it. In contrast to them, in the ^{6}Li spectrum constructed by superimposing the data on the different channels (see Fig. 11d) a structure is manifested very strongly. This could be due to the circumstance that in the partial spectra measured by the de-

tection of charged particles some information is lost because of the existence of a threshold for their detection. It is important to make measurements of the total absorption in ^{6}Li, as has been done for the neighboring nuclei.

5. Comparison of the total absorption cross sections in ^{9}Be obtained in the framework of the supermultiplet scheme (Fig. 12b) and with allowance for the complete basis (see Fig. 12a) shows that there is a fragmentation of the states described by a definite Young tableau, but complete mixing of states with different Young tableaux does not yet occur. The experimentally observed small maximum in the region of 2–10 MeV (see Fig. 10)—the pigmy resonance—is due solely to states with the Young tableau [441].

6. Basically, the theoretical curves reproduce the experimentally observed (see Fig. 10) energy dependence of the cross section and the relationships between the intensities in the different energy regions. Virtually all the experimentally observed gross structure of the excitation curve can be explained in the theory without recourse to any further assumptions or introduction of new parameters.

7. From 25 MeV (see Fig. 10) one can establish a direct connection between the energy dependence of the absorption cross section of γ rays in ^{7}Li and ^{9}Be with the cross section in ^{4}He; they appear to repeat one another.[46] In other words, in these nuclei the photoabsorption mechanism at these energies corresponds to quasi-α-particle absorption. In the nucleus ^{6}Li, the similarity commences at 30 MeV, and in nuclei of the $1p$ shell heavier than ^{7}Li and ^{9}Be at energies $E \gtrsim 40$–50 MeV, where the direct mechanism of photoabsorption must basically correspond to quasi-α-absorption. In this region, it would be interesting to carry out (γ, tp) coincidence experiments in all three nuclei and compare the angular and energy characteristics.

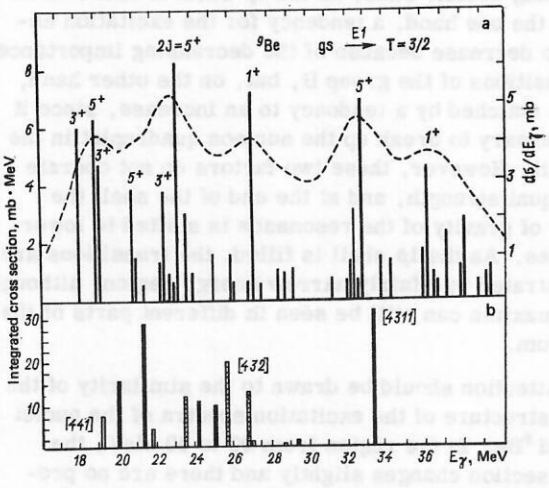

FIG. 12. Comparison of calculated photoexcitation spectra of the nucleus ^{9}Be: a) in the complex scheme[78,81] with allowance for all $1\hbar\omega$ excitations (only the $T_>=3/2$ branch of the resonance is shown), b) in the supermultiplet scheme.[42] The right-hand scale corresponds to the broken curve, which indicates the width of each level.

Decay of photonuclear resonances. As we have already noted, the partial spectra carry information about the nature of the states forming a giant resonance. It is this information that is needed for the experimental observation of configuration splitting. However, we shall begin our discussion of the partial spectra not with the nuclei in which the $1p$ shell is only beginning to be filled and the effect of splitting is most strongly manifested, but with ^{12}C. In this nucleus, the part played by the $0s$ nucleons in forming the resonance is small, and, moreover, the corresponding small maximum is situated very high. If one uses γ rays with an upper limit of the spectrum not higher than 30 MeV, the $0s$ hole states will hardly be manifested at all. As follows from such measurements,[99] in almost 90% of the cases the final ^{11}Be and ^{11}C nuclei are formed in the ground state. If we also take into account the partial cross sections to the low-lying states of the nuclei ^{11}Be and ^{11}C, in which the $0s$ shell is completely filled, this fraction reaches 98%. Such is the picture when the transitions of the group B are eliminated or have a low intensity. We now turn to nuclei in which the configuration splitting is greater. We begin with ^{6}Li.

1. Splitting in ^{6}Li. The decay scheme of the photonuclear resonance in ^{6}Li (Fig. 13) was predicted originally in the diagonal approximation.[10] Subsequent calculations only served to make the details more precise. A list of the experimental data on the various photodisintegration channels of ^{6}Li is given in Table V.

Among the states of the final nucleus in the case of ^{5}He and ^{5}Li, only the ground and first excited $J^\pi=\frac{1}{2}^-$ states are described by a configuration $(0s^4 1p)$ in which the $0s$ shell is closed. Altogether 35% of the transitions correspond to this group of levels (cf. ^{12}C). Experimentally, a transition to one further $3/2^+$ state of the ^{5}He and ^{5}Li final nuclei has been observed. These are well identified levels lying just above the threshold of their subsequent decay through the channels $d+t$ and $d+{}^3$He, respectively. The dominant component of the wave function of these states is $0s^3 1p^2[32]^4 S_{3/2^+}$. The total intensity of the transitions to this level is only two times less than the intensity of the transitions to the group of low-lying states. The remaining posi-

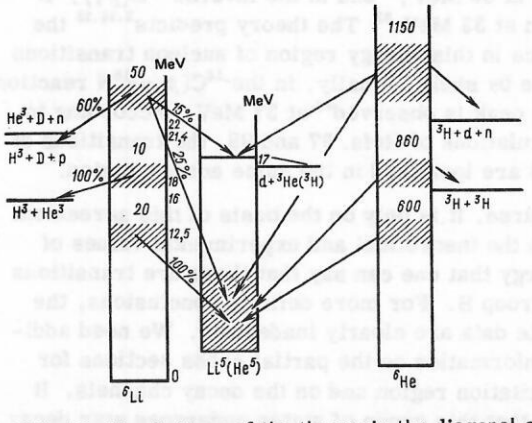

FIG. 13. Predictions of the theory in the diagonal approximation of the excitation and decay scheme of the nucleus ^{6}Li in the case of the absorption of γ rays[10,18] and muons.[31]

TABLE V. Photodisintegration channels of the nucleus ^{6}Li (experiment).

Reaction	Interval of γ-ray energies of the upper limit, MeV	Integrated cross section, mb · MeV	Fraction in the total absorption for the interval $E_\gamma \leqslant 50$ MeV, %	Reference
(γ, pn) $(\gamma, p_0)\ ^5\mathrm{He}\ (3/2^-) \to n + {}^4\mathrm{He}$ $(\gamma, p_1)\ ^5\mathrm{He}\ (1/2^-) \to n + {}^4\mathrm{He}$ $(\gamma, n_0)\ ^5\mathrm{Li}\ (3/2^-) \to p + {}^4\mathrm{He}$ $(\gamma, n_1)\ ^5\mathrm{Li}\ (1/2^-) \to p + {}^4\mathrm{He}$	50	33.5	35	18
$(\gamma, n) + (\gamma, pn)$	32	27.3		85
$(\gamma, p_0)\ ^5\mathrm{He}\ (3/2^-) \to n + {}^4\mathrm{He}$ $(\gamma, p_1)\ ^5\mathrm{He}\ (1/2^-) \to n + {}^4\mathrm{He}$	30	17.3±3.5		87
$(\gamma, t)\ ^3\mathrm{He}$	32 $25 \leqslant E_\gamma \leqslant 50$ 50 32 70 30	12.8±1.9 2.7±1.3 15±2 17±1 21±1 ≈ 7.0±1.0	16	86 87 87 100 100 101
$(\gamma, p_2)\ ^5\mathrm{He}\ (3/2^+) \to d + t$	$25 \leqslant E_\gamma \leqslant 45$	9.0±1.0		87
(γ, pdt) *	$35 \leqslant E_\gamma \leqslant 50$ 32 50	8±2 18.2±2.0 34±4	35	87 86 87
$(\gamma, n_2)\ ^5\mathrm{Li}\ (3/2^+) \to d + {}^3\mathrm{He}$	$30 \leqslant E_\gamma \leqslant 50$	9	9	87
$\gamma, 2pnt$ $\gamma, 2np\ ^3\mathrm{He}$	$35 \leqslant E_\gamma \leqslant 50$	~ 5	5	87
Total disintegration cross section	50	97±12	100	87
$\sigma_{int}(\gamma, xn)$	97	95±8		38

*The channel $nd\ ^3$He is suppressed in the entire range of energies E_γ up to 50 MeV.

tive-parity levels in the ^{5}He and ^{5}Li nuclei have higher energies. It is difficult to separate the transitions to them (on the one hand, they are not well identified, and on the other, they must have a large width due to their subsequent decay) and this has not yet been done. Evidently, these states can be regarded directly as a continuum of quasi-α-absorption and combined with the channel of disintegration into three fragments ($n + d + {}^3$He and $p + d + t$). This last channel together with $^6\mathrm{Li}^* \to {}^3\mathrm{He} + t$ makes up the remaining 50% of the intensity.

According to the measurements of Ref. 86 with ^{6}Li-enriched photographic emulsions, a group of states localized in the region of 25 MeV decay predominantly through the pdt channel. Following measurements[87] at larger values of $E_\gamma^{\max}$ revealed one further region (around 40 MeV) of localization of states that decay partly through the pdt channel. But, on the other hand, as is emphasized in Ref. 87, the symmetric nd^3He channel, which, according to theoretical estimates, should be manifested with the same intensity as the pdt channel, is suppressed. As yet, this result has not been interpreted.

We now consider the ^{6}Li(γ, ^{3}He)t channel. Experimental data on this channel are given in Fig. 14. A calculation in the framework of the shell model always leads to a single maximum, which is shown in Fig. 14d. The various authors give only different intensities for it (Refs. 10, 28, 39, and 40). In the quoted papers, the

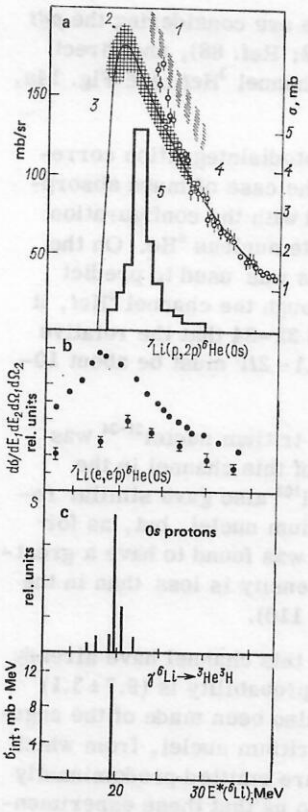

FIG. 14. Experimental data on the channel ^{6}Li(γ,t)^{3}He (a): 1) Ref. 102, 2) Ref. 103, 3) the result of calculation[104] in the framework of a cluster model, 4) Ref. 100, and 5) Ref. 86; b) the experimental excitation spectra of the nucleus ^{6}He for quasielastic proton knockout from the 0s shell in the (p,2p) reaction[7,8] and (e,$e'p$) reaction[105]; c) the spectroscopic factors for separation of a 0s proton in ^{7}Li (the calculation of Ref. 28); d) the channel ^{6}Li(γ,t)^{3}He in the framework of the resonance mechanism (Refs. 10, 28, 39, and 40).

energy position of the peak served as the point of reference for the complete scale of levels forming the giant resonance. Measurements in the (p,2p) reaction on ^{7}Li provided the basis for this. It so happens that the knockout of 0s nucleons leads to predominant population of the $J^\pi, T = 2^-, 1$ state of the nucleus ^{6}He that is responsible for the decay in the photoabsorption reaction on ^{3}Het. The corresponding distribution of the spectroscopic factors for 0s-nucleon knockout[28] is given in Fig. 14c. It followed from the first experiments on (p,2p) knockout that in ^{6}Li the level in which we are interested is situated somewhere in the region of 17 MeV.[78,106] Subsequent measurements with better resolution,[103,107] and also the data[105] obtained from the ^{7}Li(e,$e'p$) reaction, showed that the maximum is in the region 20–21 MeV (see Fig. 14b), which also agrees well with the result obtained from photodisintegration.[86]

As follows from the analysis of the proton quasielastic knockout reaction and the photodisintegration of ^{6}Li through the channel ^{3}Het, the real situation is that the level which collects the maximal intensity has a very large width of the order of a few MeV. A similar situation is realized for all the remaining levels that form the dipole resonance in ^{6}Li. Therefore, a more realistic calculation must be based on the quasi-α-particle

mechanism of absorption if we are considering the *pdt* channel (see Fig. 11d, curve 2; Ref. 88), and direct disintegration[104] through the channel ^{3}He*t* (see Fig. 14a, curve 3).

The channel ^{3}He*t* for ^{6}Li photodisintegration corresponds[34] to the 2*t* channel in the case of muon absorption, which is also associated with the configuration $|0s^3 1p^3[33]\rangle$ of the intermediate nucleus ^{6}He. On the basis of the same approach as was used to predict photodisintegration of ^{6}Li through the channel ^{3}He*t*, it was predicted in Refs. 31 and 32–34 that the relative probability of the channel $\mu^6\text{Li} \to 2t\nu$ must be about 10–15%.

The calculated spectrum of tritium nuclei[31-34] was found to be very soft. Study of this channel in the framework of a cluster model[109] also gave similar results for the spectrum of tritium nuclei, but, as for the photonuclear reaction, it was found to have a greater spread. The predicted intensity is less than in the first approach (see also Ref. 110).

First experimental data on this channel have already been obtained.[111] It relative probability is $(9.7 \pm 3.1) \times 10^{-2}$. Measurements have also been made of the angular correlation between the tritium nuclei, from which it follows that the particles are emitted predominantly at large angles. It appears to us that these experimental data, together with the photonuclear data, will stimulate new systematic calculations of this channel.

The coincidence method has now started to be used to study the disintegration channels of ^{6}Li with the emission of charged particles.[101,102] In investigations of this kind, it is important to have particle detection thresholds as low as possible, since, as a rule, the emitted fragments have low energies. In Ref. 112, the reaction $^6\text{Li}(\gamma, ab)X$ with emission of charged particles *a* and *b* detected in coincidence in the range $E_\gamma \leq 55$ MeV of the γ-ray energies was studied. The majority of these reactions were $^6\text{Li}(\gamma, pt)X$ (the detection thresholds were 3 MeV for the protons, 3.5 MeV for the deuterons, 4 MeV for the tritium nuclei, and 10 MeV for the nuclei ^{3}He and ^{4}He). The correlation between the emission directions and the energy distributions of the protons and the tritium nuclei were measured. These results were analyzed under the assumption of a quasi-α-particle mechanism of ^{6}Li disintegration. The cross section was expressed in the form

$$d\sigma_{ab}(\theta, E_\gamma)/dE_a\, d\Omega_1\, d\Omega_2 \sim \rho(E_\gamma) \mid \Phi(q) \mid^2 (d\sigma_{ab}/d\Omega)_{^4\text{He}}, \qquad (21)$$

where $\rho(E_\gamma)$ is the density of the final states per unit energy interval, $\Phi(q)$ is the function which describes the momentum distribution of the α cluster in the nucleus, and $(d\sigma_{ab}/d\Omega)_{^4\text{He}}$ is the differential cross section of ^{4}He photodisintegration into the particles *a* and *b* at the energy E_γ. The obtained calculated curve for the proton yield was normalized by the corresponding experimental curve at an aribtrary point. The results of the calculation and the measurements are compared in Fig. 15. It was concluded on the basis of the results that the curve obtained under the assumption that the $^6\text{Li}(\gamma, pt)X$ reaction is a three-particle reaction, i.e., $^6\text{Li}(\gamma, pt)d$, does not agree with the experiment, where-

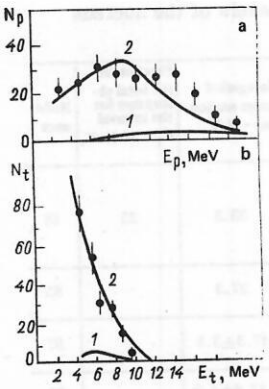

FIG. 15. Energy distribution of the protons (a) and the coincident tritium nuclei (b) in the reaction $^6\text{Li}(\gamma, pt)X$ according to the results of Ref. 112: 1) the result of calculation under the assumption of photodisintegration of α clusters for the reaction $^6\text{Li}(\gamma, pt)d$; 2) the same as 1) but for the reaction $^6\text{Li}(\gamma, pt)pn$; curve 2 in Fig. 15a is normalized to pass through the experimental points in the region of the ordinate.

as the curve constructed on the basis of a four-particle reaction, i.e., $^6\text{Li}(\gamma, pt)np$, is close to the measured curve. However, this result contradicts the results of the preceding experiments, the results of which are shown in Fig. 11d. Therefore, it is necessary to make a series of successive measurements of ^{6}Li photodisintegration through different channels, which would make it possible to establish the basic features of this process.

Summarizing our discussion of ^{6}Li photodisintegration, we should point out that, on the one hand, the available experimental data indicate the existence of configuration splitting of the photonuclear resonance in this nucleus. Moreover, they confirm the prediction made by the theory of a many-particle star nature of the disintegration of this nucleus. On the other hand, the quantitative agreement between the theory and experiment is rather poor. The existing experimental data are rather diverse, and much work is needed to establish systematically the basic features of ^{6}Li disintegration. Complete calculations of ^{6}Li photodisintegration are also not available. Here, an important point could be played by calculations based on a cluster nature of the ^{6}Li structure, as was done in Refs. 88 and 104. The Faddeev equations with forbidden states[113] could provide a good formal basis for taking into account, for example, in the $\gamma + {}^6\text{Li} \to t + d + p$ channel, the interaction of the particles in the final state. As detailed information as possible is required on the energy and angular characteristics.

2. Disintegration of ^{7}Li. The results of the theoretical[79,81] and experimental investigations of the population of the various states of the daughter nuclei ^{6}Li and ^{6}He are given in Table VI. The corresponding theoretical total absorption curve was given in Fig. 9. Overall, the calculation in the complete scheme leads to qualitatively the same picture of ^{7}Li disintegration as in the diagonal approximation. This last is shown in Fig. 16 with indication of the Young tableau of each group of levels. Also given are the experimental data on the channel $^7\text{Li}(\gamma, {}^4\text{He})t$, which determines the total

TABLE VI. Results of theoretical[79,81] and experimental* investigation of the population of the various states of the daughter nuclei ^{6}Li and ^{6}He following photodisintegration of ^{7}Li.

$J_f^\pi T_f$	Channel ^{6}Li+n				Channel ^{6}He+p			
	E^*(^{6}Li), MeV	Partial cross section		Subsequent decay	E^*(^{6}He), MeV	Partial cross section		Subsequent decay
		mb · MeV	%			mb · MeV	%	
1+0	0	7	6	—	—	—	—	—
3+0	2.18	9 $\leqslant$2.0 [a]	9	^{4}Hed	—	—	—	—
0+1	3.56	10 $\leqslant$5.0 [a] 11±3 [b]	9	γ	0	4 14.4±0.6 [c] 15 [d]	3	β
2+0	4.31	6	5	^{4}Hed	—	—	—	—
2+1	5.37	9	8	γ	1.8	6 4.0±1.4 [c]	6	^{4}He2n
1+0	5.65	1	0.5		—	—	—	—
Remaining positive-parity levels in the energy range 10–17 MeV		8	7	^{4}Henp		2	1	^{4}He2n
2−1 1−1	(19.9) ** (20.8) **	17 5	15 4	^{3}He^{3}H	(17.9) ** (18.8) **	7 1	6 1	^{3}H^{3}H
Remaining negative-parity levels		18	16			5	5	
Sum over all positive-parity states		49	43			12	10	
Sum over all negative-parity states		40	35			13	12	
Sum over all states		89	78			25	22	

*The experimental data are taken from the following papers: a) E_γ^{max}=32 MeV (Ref. 118), b) E_γ^{max}=55 MeV (Ref. 115), c) E_γ^{max}=35 MeV (Ref. 114), d) E_γ^{max}=30 MeV (Ref. 116).

**0s hole states.

cross section in the low-energy part of the spectrum. The cross section integrated over this channel is small—from 3.8 mb·MeV according to Ref. 119 to 8.1 mb·MeV.[117] Theory relates decay ^{7}Li*→^{4}He+t to a group of states with Young tableau [43]. As for the reaction ^{6}Li(γ,^{3}He)t, the theory correctly predicts the position of the maximum, but again the width of the level is so great that the spectrum is spread over a broad energy range. The estimate of this channel[117] in the framework of a simplified cluster model (broken curve in Fig. 16) does not agree well with the experimental data on the position of the maximum or the nature of the energy distribution.

As follows from the theory, the population of the positive-parity levels of the nuclei ^{6}He and ^{6}Li is associated with a state of group A, and therefore the partial cross sections repeat the low-energy part of

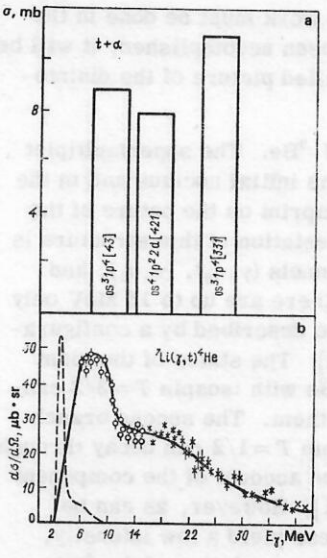

FIG. 16. Total photoabsorption cross section of ^{7}Li calculated in the diagonal approximation[9] (a) with indication of the wave-function structure of the final state; experimental data (b) on the channel ^{7}Li(γ,t)α and the result of calculation of this channel in a simplified cluster model[117] (broken curve).

the total spectrum. The population of the negative-parity levels is associated with the decay of group B. Decays to levels of different parity are divided almost equally.

The calculated integrated cross sections agree with the measured values (see Table VI), with the only exception of the channel (γ,p_0). Overall, agreement is also observed with the total yield through various channels, for which the measured integrated cross sections are given in Table VII.

Detection of two particles in coincidence in the disintegration of ^{7}Li showed that the main channels are ^{7}Li(γ,pt)t and ^{7}Li(γ,pdn)t, the latter being the stronger according to Ref. 112.

Concluding our discussion of the disintegration of ^{7}Li, we note that the available experimental data confirm the conclusions of the theory of configuration splitting of the resonance and the large part played by "star" decay of the high-lying excitations. Of course, much work must still be done on the accumulation of data on the emission of various particles in coincidence and the determination of the complete disinte-

TABLE VII. Results of experimental investigation of various disintegration channels of the nucleus ^{7}Li.

Channel	Integrated cross section, mb · MeV	E_γ^{max}, MeV	Reference
(γ, 1n)	10.1	30.5	[85]
(γ, 2n)	10.0	30.5	[85]
(γ, p2n)	13.3	23	[119]
	12.0±2.0	23—33	[119]
(γ, p)	14.0±1.5	23	[119]
(γ, pt)	22±3	52	[119]
(γ, nt)	33±4	52	[119]
	3.8	33	[119]
	8	30	[120]
(γ, $t\alpha$)	8.1	50	[117]
	4.4±0.7	28	[101]

gration scheme. The same work must be done in the theory. When this has all been accomplished, it will be possible to establish a detailed picture of the disintegration of this nucleus.

3. Disintegration of ^{9}Be. The supermultiplet structure of the levels in the initial nucleus and in the final ^{8}Be leaves a strong imprint on the nature of the decay. The clearest manifestation of this structure is the low intensity of the channels (γ,n_0), (γ,n_1), and (γ,n_2). In the nucleus ^{8}Be there are up to 16 MeV only levels with $T=0$, which are described by a configuration with Young tableau [44]. The states of the giant resonance of the nucleus ^{9}Be with isospin $T=3/2$ cannot, of course, decay into them. The second branch of the resonance with isospin $T=1/2$ can decay through these three channels only on account of the component with the Young tableau [441]. However, as can be clearly seen in Fig. 12, these yield a low intensity, which explains the very weak population of the first three states of the nucleus ^{8}Be. The experimental data (see Ref. 121) completely corresponds to this conclusion of the theory.

The strongest channels are the ones leading to population of the states of the ^{8}Be nucleus beginning at 16 MeV. Because of this feature of the decay, the part played by the channels with the emission of $\alpha+{}^5$He and $d+{}^7$Li fragments is more important. The cross sections calculated[42] for these channels are shown in Fig. 17 together with the experimental data. Good agreement between the theory and experiment is observed.

4. Disintegration of the remaining nuclei of the $1p$ shell. As the $1p$ shell is filled, the importance of the group B decreases, and the decay of the resonance is associated with population of the ground state of the final $A-1$ nucleus and the states with the same parity as the ground state. The example of the decay of the resonance in ^{12}C already considered illustrates how this change in the structure of the state actually occurs. As is shown by the analysis of Ref. 79, the picture is the same in all the following nuclei, namely, there is population of states of the same nature as the ground state of the final nucleus.

On the other hand, the group B does not disappear completely. This follows from the theory. Moreover, there are some experimental indications of the manifestation of this group. As was shown in Ref. 12, the distinctive feature of this group is the star decay. Thus, in ^{12}C the group B is formed from states with Young tableau [4431], and their decay leads to the emission of $2\alpha+t+p$ or $2\alpha+n+{}^3$He fragments. In ^{14}N, they are states with Young tableau [4433], whose decay leads to the formation of $2\alpha+t+{}^3$He fragments The identification of such channels requires a special experiment. We believe that such experiments would be of interest and that their results could give important information about the nature of the hole excitations of light nuclei.

Magnetic quadrupole excitations in inelastic electron scattering and the radiative capture of π mesons. Transverse E1 *excitations.* 1. We begin the discussion of the excitation of an intermediate nucleus in the backward scattering of electrons ($M2$ and $E1t$ transitions), the radiative capture of π mesons, and μ capture with the ^{16}O nucleus with closed shells. The theoretical[57] and experimental[123,124] excitation spectra in the various reactions are given in Fig. 18. According to the calculations, the $M2$ transitions in electron scattering are grouped in three energy regions, which is a consequence of the spin–orbit forces, which lead to configuration splitting. The greatest intensity is associated with the transition $1p_{3/2}\to 2d_{5/2}$. The two outside maxima are manifested much less strongly. Measurements of the inelastic scattering of electrons

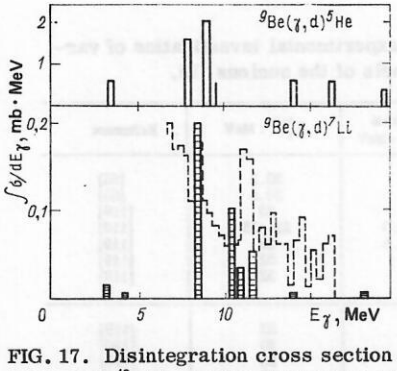

FIG. 17. Disintegration cross section of ^{9}Be with emission of fragments.[42] The broken histogram is the result of the measurements of Ref. 122.

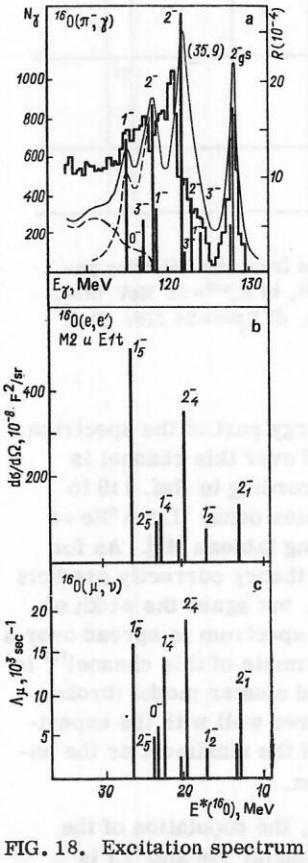

FIG. 18. Excitation spectrum of the nuclear system in the case of radiative capture of pions (a), electron scattering (b), and absorption of muons by the nucleus ^{16}O (c): the theory of Ref. 57 and the experiment of Ref. 123.

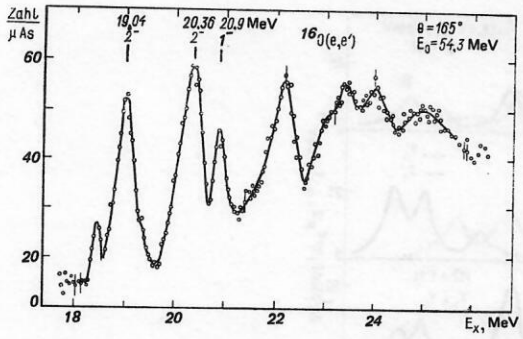

FIG. 19. Excitation spectrum of the nucleus ^{16}O in the case of electron scattering[124] through 165°.

indicate the presence of a peak in the region of 20 MeV (true, it is split) due to excitation of $J^\pi T = 2^-1$ states (Fig. 19).

In the $^{16}O(\pi^-,\gamma)$ reaction, the $M2$ resonance and its splitting are manifested more clearly in the theoretical curve, since the outer peaks collect a somewhat greater intensity. Analysis of the excitation spectra of the nucleus ^{16}O in the $^{16}O(\pi,\gamma)$ and $^{16}O(e,e')$ reactions revealed a number of peaks (Table VIII), which correlate in energy well with each other and with the result of the theoretical calculation shown in Fig. 18. In particular, good agreement is observed in the position of the $J^\pi T = 2^-1$ levels that form the $M2$ resonance and the splitting of the resonance. A similar correlation can be established[126,128] in the nucleus ^{12}C.

The transverse $E1$ excitations in the $^{16}O(e,e')$ reaction are concentrated in the region of 25 MeV in one level, with the consequence that in the total excitation spectrum of the nucleus in the case of backward scattering of low-energy electrons, which is the sum of $M2$ and $E1t$ transitions, the energy region 20–25 MeV collects an appreciable fraction of the excitation intensity. Indeed, in the measured cross section of inelastic electron scattering in this region of excitation energies a broad maximum is observed[123] (see Fig. 19), this being due in large measure to $E1t$ transitions.[125]

The absorption of muons leads to the excitation to equal extent of the states $J^\pi T = 2^-1$ and 1^-1, as in the case of electron scattering. Concluding our discussion of the nucleus ^{16}O, we emphasize that in this nucleus with closed shells the available experimental data confirm the concept of configuration splitting.

TABLE VIII. Structure of the excitation spectrum of the nuclear system revealed in the $^{16}O(\pi^-,\gamma)$ and $^{16}O(e,e')$ reactions.

^{16}O (π, γ) [123]				^{16}O (e, e') [124]		
E_γ, MeV	E^* (^{16}N), MeV	E^* (^{16}O), MeV	$R_\gamma \cdot 10^4$	E^* (^{16}O), MeV	J^π	$B(M\,2.0)$, F^4
128.0	0	12.98	14.5±0.6	12.98	2⁻	
123.9	4.1±0.2	17.1±0.2	2.3±0.4	17.14	1⁻	
123.2	4.8±0.2	17.7±0.2	2.4±0.4	17.6	2⁻	0.26
121.7	6.1±0.2	19.0±0.2	4.4±0.6	19.04	2⁻	3.6
120.5				19.5	1⁻	
120.5	7.5±0.2	20.4±0.2	15.1±0.6	20.36	2⁻	5.1
118.8	9.1±0.2	22.2±0.2	9.3±1.2	22.3	1⁻	
116.9	11.1±0.2	24.0±0.2	5.8±0.8	24.2	1⁻	
115.8	12.2±0.2	25.2±0.2	2.9±0.6			
114.5	13.5±0.2	26.4±0.2	3.6±0.6			

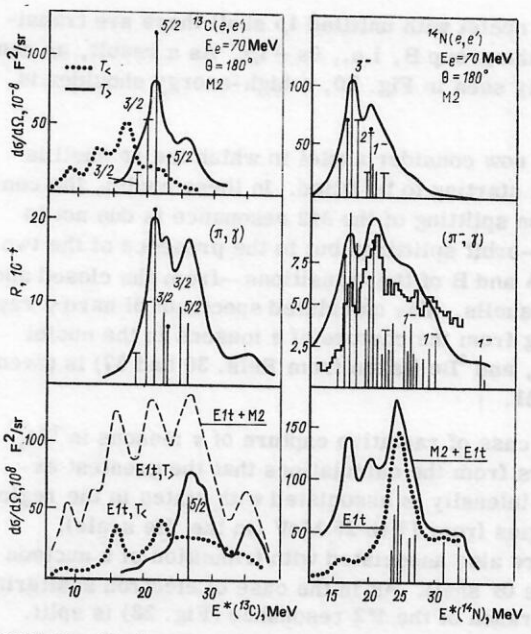

FIG. 20. Excitation spectrum of the nuclear system in the case of backward electron scattering and radiative capture of π mesons by the nuclei ^{13}C and ^{14}N: the theory of Ref. 57 and the experiment (histogram) of Ref. 126.

2. As the number of nucleons in the $1p_{1/2}$ shell decreases, its contribution to the resonance becomes weaker. Therefore, the low-energy branch of the $M2$ resonance associated with it also becomes weaker. The splitting between the two groups of the transitions $1p_{3/2} \to 2d_{5/2}$ and $1p_{3/2} \to 2d_{3/2}$ remains, despite the fact that the localization region of the first is significantly broadened in nuclei with shells that are not closed. As a result, the excitation spectrum of the nucleus due to the $M2$ transitions (in the case of electron scattering and radiative capture of π mesons) has two humps. This can be clearly seen in Fig. 20 in the calculated[30,57] excitation spectra of the nuclei ^{13}C and ^{14}N. The structure of the states that form the resonance in the (π,γ) reaction in ^{13}C and ^{14}N is given in Table IX.

The measured[126,127] spectra of hard γ rays from the radiative capture of π mesons by the same nuclei also reveals a two-hump nature of the excitation curve (see the histogram in Fig. 20).

The transverse $E1$ excitations are again sharply concentrated in the same energy region as in ^{16}O. How-

TABLE IX. Structure of the states forming the $M2$ resonance in the nuclei ^{13}C and ^{14}N.

Nucleus	J^π	E^*, MeV	Weight of component, % $2d_{5/2}$	$2s$	$2d_{3/2}$	Nucleus	J^π	E^*, MeV	Weight of component, % $2d_{5/2}$	$2s$	$2d_{3/2}$
^{14}N	2⁻	14.5	89	5	6	^{14}N	1⁻	22.0	15	33	52
	3⁻	14.9	47	22	31		1⁻	23.8	50	5	45
	3⁻	15.9	41	7	52						
	2⁻	11.7	63	32	5						
	2⁻	18.3	85	6	9		3/2⁺	5.5	34	64	0
	3⁻	18.6	53	9	38		5/2⁺	6.4	67	29	0
	3⁻	20.1	59	7	44		3/2⁺	8.0	56	41	0
	2⁻	21.3	35	11	55	^{13}C	5/2⁺	8.5	36	52	12
	2⁻	21.7	45	32	23		3/2⁺	10.6	36	14	50
							5/2⁺	11.6	47	4	50
							1/2⁺	11.9	9	42	49

ever, in nuclei with unfilled $1p$ shell there are transitions of the group B, i.e., $0s \to 1p$. As a result, as can be clearly seen in Fig. 20, a high-energy shoulder is formed.

3. We now consider nuclei in which the $1p$ shell is only just starting to be filled. In these nuclei, the configuration splitting of the $M2$ resonance is due not to the spin–orbit splittings but to the presence of the two groups A and B of the transitions—from the closed and valence shells. The calculated spectrum of hard γ rays resulting from the capture of π mesons in the nuclei ^{6}Li, ^{7}Li, and ^{9}Be (taken from Refs. 30 and 57) is given in Fig. 21.

In the case of radiative capture of π mesons in ^{7}Li, it follows from the calculations that the greatest excitation intensity is associated with states in the region of energies from 17 to 25 MeV (in the ^{7}He scale), which are also associated with transition of a nucleon from the $0s$ shell. As in the case of electron scattering, the $T_>$ branch of the $M2$ resonance (Fig. 22) is split. The excitation curves almost repeat one another. In the $E1t$ excitations, the group A is manifested weakly and almost the entire strength of the transitions is concentrated on group B.

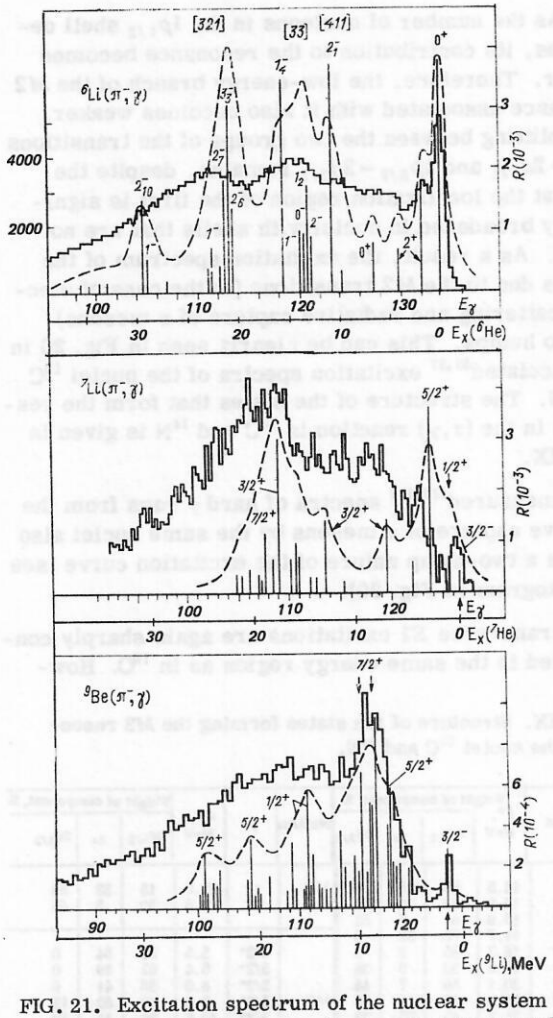

FIG. 21. Excitation spectrum of the nuclear system in the radiative capture of π mesons by nuclei of the Li and Be isotopes: the theory of Ref. 30 and the experiment (histogram) of Refs. 126 and 127.

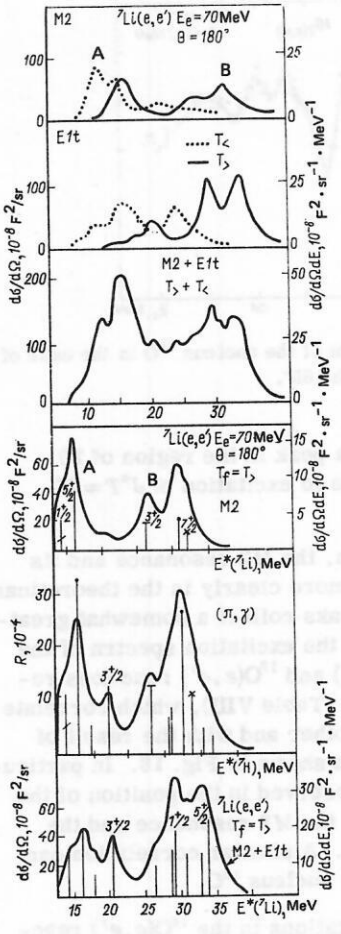

FIG. 22. Excitation spectrum of the nuclear system in the case of backward electron scattering and radiative capture of π mesons by the nucleus ^{7}Li (theory of Ref. 30).

In ^{9}Be, strong transitions in the (π,γ) reaction from the $0s$ shell are concentrated on levels situated above 15 MeV. However, they are not so strong as in the Li isotopes. The strongest transitions—in the (π,γ) reaction and in the case of $M2$ excitations as a result of electron scattering—are the transitions in which $1p$ nucleons are excited. Conversely, the transverse $E1$ excitations are due predominantly to transitions of nucleons from the $0s$ shell (Fig. 23).

Thus, in $M2$ excitations we observe the following picture as the $1p$ shell is filled: a decrease in the intensity of the transitions of nucleons from the $0s$ shell (group B), an enhancement of those from the $1p$ shell (group A), and a softening of the excitation spectrum of the nucleus—in complete analogy with photonuclear reactions.

Beginning with ^{9}Be and in all the following nuclei the most intense transition is an $M2$ transition in which the spin of the nucleus changes by two units: $\Delta J = 2$. The Li isotopes are an exception, and this is due to the existence of additional selection rules which arise because of the realization of the supermultiplet level scheme. As a result of this, the orbital component, which gives the dipole transitions, has selection rules that restrict the possible values of the orbital angular

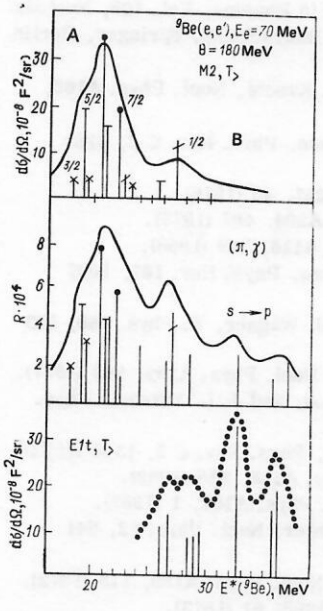

FIG. 23. Excitation spectrum of the nuclear system in the case of backward electron scattering and radiative capture of π mesons by the nucleus ^{9}Be (theory of Ref. 30).

momentum of the final state.[30] For example, in the group of levels with the Young tableau [33] transitions from the ground state $0s^4 1p^2[42]^{13}S$ proceed only to states with the configuration $|0s^3 1p^3[33]^{33}P\rangle$. Therefore, the total angular momentum of the state cannot take the value $J_f = J_i + 2 = 3$. Only the high-energy group of levels can contain the configuration $|0s^3 1p^3[321]^{35}P\rangle$, in which the angular momentum $J_f = 3$ is realized. In ^{7}Li, the situation is similar; there, the states with spin $J_f^\pi = 7/2^+$ play a small part in the formation of the resonance.

Conversely, the transverse $E1$ excitations in nuclei at the start of the $1p$ shell form the resonance predominantly from transitions of group B. Group A is manifested much more weakly, and therefore the resonance is at high energies. Calculations confirm the decisive role of configuration splitting in the formation of the gross structure of excitation spectra of the nuclei at the start of the $1p$ shell in the case of radiative capture of π mesons and electron scattering. The available experimental data [basically on the (π,γ) reaction] find a natural explanation in the framework of such splitting. With regard to the inelastic electron-scattering reaction, $M2$ transitions have, as we said above, been found so far in ^{12}C and ^{16}O.

Recently, there have been indications[129] that the maximum in ^{14}N at 16.1 MeV also corresponds to $M2$ excitation. As yet, the situation is not sufficiently definite for one to be able to speak with confidence of an $M2$ resonance on the basis of the available data on electron scattering.

As follows from what we have said, the π-meson radiative-capture reaction (together with inelastic electron scattering) is a good tool for studying magnetic quadrupole transitions. Comparison of the results of measurements of both reactions will complement the information on the part played by the $M2$ resonance in nuclei of the $1p$ shell and reveal the basic features of its excitation.

[1]A. B. Migdal, Zh. Eksp. Teor. Fiz. 15, 81 (1945).
[2]M. Goldhaber and E. Teller, Phys. Rev. 74, 1046 (1949).
[3]D. Wilkinson, Physica (Utrecht) 22, 1039 (1956).
[4]G. E. Brown, Unified Theory of Nuclear Models and Forces, 2nd Ed., North–Holland (1967) [Russian translation published by Atomizdat, Moscow (1970)].
[5]V. V. Balashov, V. G. Shevchenko, and N. P. Yudin, Zh. Eksp. Teor. Fiz. 41, 1929 (1961) [Sov. Phys. JETP 14, 1371 (1962)].
[6]S. Dehesa, in: Lecture Notes in Physics, Vol. 61, Springer, Berlin.
[7]L. A. Malov and V. G. Solov'ev, Fiz. Elem. Chastits At. Yadra 11, 301 (1980) [Sov. J. Part. Nucl. 11, 111 (1980)].
[8]In: Trudy IV seminara: Élektromagnitnye vzaimodeĭstviya yader pri malykh i srednikh énergiyakh (Proc. Fourth Seminar: Electromagnetic Interactions of Nuclei at Low and Medium Energies), Nauka, Moscow (1979).
[9]V. G. Neudachin, V. G. Shevchenko, and N. P. Yudin, in: Trudy tret'eĭ Vsesoyuz. konferentsii po yadernym reaktsiyam pri malikh i srednikh énergiyakh, 1960 (Proc. Third All-Union Conf. on Nuclear Reactions at Low and Medium Energies, 1960), Izd. Akad. Nauk SSSR (1962).
[10]V. V. Balashov and R. A. Éramzhyan, in: Tezisy XIV Vsesoyuz. soveshchaniya po yadernoĭ spektroskopii i strukture atomnogo yadra (Proc. 14th All-Union Symposium on Nuclear Spectroscopy and Nuclear Structure); R. A. Éramzhyan, Izv. Akad. Nauk SSSR, Ser. Fiz. 28, 1181 (1964).
[11]V. G. Neudatchin and V. N. Orlin, Nucl. Phys. 31, 338 (1962).
[12]V. G. Neudachin, V. G. Shevchenko, and N. P. Yudin, Phys. Lett. 10, 180 (1964).
[13]V. G. Neudatchin and Yu. F. Smirnov, Nucl. Phys. 66, 25 (1965).
[14]Trudy Mezhdunarodnoĭ konferentsii po élektromagnitnym vzaimodeĭstviyam pri nizkikh i srednikh énergiyakh (Proc. Intern. Conf. on Electromagnetic Interactions at Low and Medium Energies), Vol. 3, Moscow (1967), p. 351.
[15]V. G. Shevchenko, ibid., p. 206.
[16]A. P. Komar and E. D. Makhnovskiĭ, Dokl. Akad. Nauk SSSR 156, 774 (1964) [Sov. Phys. Dokl. 9, 463 (1964)].
[17]E. B. Bazhanov, A. P. Komar, and A. V. Kulikov, Zh. Eksp. Teor. Fiz. 46, 1496 (1964) [Sov. Phys. JETP 19, 1013 (1964)].
[18]E. B. Bazhanov *et al.*, Nucl. Phys. 68, 191 (1965).
[19]V. P. Denisov *et al.*, Yad. Fiz. 5, 498 (1967) [Sov. J. Nucl. Phys. 5, 349 (1966)].
[20]V. G. Neudatchin and V. G. Shevchenko, Phys. Lett. 12, 18 (1964).
[21]V. V. Varlamov *et al.*, Yad. Fiz. 28, 590 (1978) [Sov. J. Nucl. Phys. 28, 302 (1978)].
[22]B. S. Ishkhanov *et al.*, Nucl. Phys. A313, 317 (1979).
[23]V. V. Varlamov *et al.*, Izv. Akad. Nauk SSSR, Ser. Fiz. 43, 186 (1979).
[24]V. V. Varlamov *et al.*, Yad. Fiz. 30, 1185 (1979) [Sov. J. Nucl. Phys. 30, 617 (1979)].
[25]L. Majling *et al.*, Nucl. Phys. A143, 429 (1970).
[26]V. V. Balashov, G. Ya. Korenman, and R. A. Éramzhyan, Pogloshchenie mezonov atomnymi yadrami (Absorption of Mesons by Nuclei), Atomizdat, Moscow (1978).
[27]Yu. I. Bely *et al.*, Nucl. Phys. A204, 357 (1973).
[28]R. A. Sakaev and R. A. Éramzhyan, Soobshcheniya (Communication) R2-9610 [in Russian], JINR, Dubna (1976).
[29]R. A. Eramzhyan, L. Majling, and J. Rizek, Nucl. Phys. A247, 411 (1975).
[30]H. R. Kissener *et al.*, Nucl. Phys. A312, 394 (1978); Communication E2-11275, JINR, Dubna (1978); M. Gmitro *et al.*, in: Mikroskopicheskie raschety struktury yadra i yadernykh reaktsiĭ (Microscopic Calculations of Nuclear Structure and Nuclear Reactions), Shtiintsa, Kishinev (1980), p. 3.
[31]V. A. Vartanyan and R. A. Éramzhyan, Voprosy atomnoĭ

nauki i tekhniki. Seriya: fizika vysokikh énergii i atomnogo yadra (Problems of Atomic Science and Technology. Series: High-Energy and Nuclear Physics), Khar'kov, No. 1(3), 25 (1973).
[32]Yu. A. Batusov and R. A. Éramzhyan, Fiz. Elem. Chastits At. Yadra 8, 229 (1977) [Sov. J. Part. Nucl. 8, 95 (1977)].
[33]V. V. Balashov, G. Ya. Korenman, and R. A. Éramzhyan, Fiz. Elem. Chastits At. Yadra 4, 585 (1973) [Sov. J. Part. Nucl. 4, 247 (1973)].
[34]V. V. Balashov and R. A. Éramzhyan, in: Materialy IV zimnei shkoly po teorii yadra i fizike vysokikh énergii, Leningrad (Proc. Fourth Winter School on Nuclear Theory and High Energy Physics, Leningrad), A. F. Ioffe Physico-Technical Institute (1969), p. 169; V. V. Balashov *et al.*, Preprint E4-4601, JINR, Dubna (1969); in: Proc. Third Intern. Conf. on High Energy Physics and Nuclear Structure (ed. S. Devons), Plenum Press, New York (1970), p. 174.
[35]R. A. Eramzhyan, L. Majling, and L. Řizek, Czech. J. Phys.; E2-80-603, JINR, Dubna (1980).
[36]L. Majling *et al.*, in: Proc. Kaon Factory Workshop, TRIUMF, Vancouver (1979), p. 141; Phys. Lett. B92, 256 (1980).
[37]V. G. Neudachin and Yu. F. Smirnov, Nuklonnye assotsiatsii v legkikh yadrakh (Nucleon Associations in Light Nuclei), Nauka, Moscow (1969); V. G. Neudatchin and Yu. F. Smirnov, in: Progress in Nuclear Physics (eds. D. M. Brink and M. A. Mulvey), Vol. 10, Pergamon Press (1969), p. 273.
[38]A. N. Boyarkina, Struktura yader 1*p*-obolochki (Structure of Nuclei of the 1*p* Shell), Moscow State University (1973); Izv. Akad. Nauk SSSR, Ser. Fiz. 28, 337 (1964).
[39]I. V. Kurdyumov *et al.*, Izv. Akad. Nauk SSSR, Ser. Fiz. 30, 292 (1966).
[40]I. V. Kurdyumov *et al.*, Phys. Lett. B31, (1970).
[41]S. Costa, S. Ferroni, V. Wataghin, and R. Malvano, Phys. Lett. 4, 308 (1963).
[42]M. J. Jacobsen, Phys. Rev. 123, 229 (1961); B. Čujec, Nucl. Phys. 37, 396 (1962); F. C. Barker, Nucl. Phys. 83, 418 (1966); L. Majling, V. I. Kukulin, and Yu. F. Smirnov, Czech. J. Phys. B18, 1563 (1968); Phys. Lett. 27, 487 (1968).
[43]D. M. Brink, in: Intern. School of Physics Enrico Fermi 36, 247 (1966).
[44]Y. Abe and N. Takigawa, Prog. Theor. Phys. Suppl. 52, 228 (1972).
[45]M. Demeur and G. Reidemeister, Ann. Phys. (N.Y.) 1, 181 (1966).
[46]A. S. Cherkasov, Yad. Fiz. 28, (1978) [Sov. J. Nucl. Phys. 28, 328 (1978)].
[47]W. Bassichis and F. Scheck, Phys. Rev. 145, 771 (1966).
[48]S. T. Belyaev, Collective Excitations in Nuclei, Gordon and Breach, New York (1967).
[49]V. G. Shevchenko and N. P. Yudin, At. Energy Rev. (Vienna) 3, 3 (1965).
[50]R. A. Éramzhyan, Dissertation [in Russian], JINR, Dubna (1976).
[51]J. E. M. Thomson, M. N. Thomson, and R. J. Stewart, Nucl. Phys. A290, 14 (1977).
[52]V. P. Denisov, Preprint No. 96 [in Russian], Leningrad Institute of Nuclear Physics (1974).
[53]J. G. Woodworth *et al.*, Nucl. Phys. A327, 53 (1979).
[54]J. W. Juri, C. K. Ross, and V. K. Sherman, Nucl. Phys. A337, 503 (1980).
[55]Kaon-Yadernoe vzaimodeĭstvie i giperyadra (Kaon—Nucleus Interaction and Hypernuclei), Nauka, Moscow (1979).
[56]W. Bruckner *et al.*, in: Proc. of the Kaon Factory Workshop, TRIUMF, Vancouver (1979), p. 124.
[57]R. A. Eramzhyan, M. Gmitro, and H. R. Kissener, Nucl. Phys. A338, 436 (1980).
[58]S. Cohen and D. Kurath, Nucl. Phys. A73, 1 (1965).
[59]G. Jacob and Th. A. J. Maris, Rev. Mod. Phys. 45, 6 (1973).
[60]Th. A. J. Maris, in: Proc. Fifth Intern. Conf. on High Energy Physics and Nuclear Structure, Amsterdam (1974).
[61]J. Mougey, in: Lecture Notes in Physics, Vol. 108, Nuclear Physics with Electromagnetic Interactions, Springer, Berlin (1979), p. 356.
[62]E. Krämer, G. Mairle, and G. Kaschl, Nucl. Phys. A165, 353 (1971).
[63]R. O. Nelson and N. R. Roberson, Phys. Rev. C 6, 2153 (1972).
[64]J. D. Sherman, Nucl. Phys. A257, 45 (1976).
[65]J. Jänecke *et al.*, Nucl. Phys. A204, 497 (1973).
[66]H. E. Gove *et al.*, Nucl. Phys. A116, 369 (1968).
[67]B. H. Wildenthal and E. Newman, Phys. Rev. 167, 1027 (1968).
[68]H. Mackh, G. Mairle, and G. J. Wagner, Z. Phys. 269, 353 (1974).
[69]R. E. Tribble and K.-I. Kubo, Nucl. Phys. A282, 269 (1977).
[70]R. C. Bearse, D. H. Youngblood, and J. L. Yntema, Phys. Rev. 167, 1043 (1968).
[71]T. G. Dzubay and R. V. Poore, Phys. Rev. C 5, 1304 (1972).
[72]G. T. Kaschl *et al.*, Nucl. Phys. A136, 286 (1969).
[73]S. Cohen and D. Kurath, Nucl. Phys. A101, 1 (1967).
[74]W. T. Pinkston and G. R. Satchler, Nucl. Phys. 72, 641 (1965).
[75]U. Wille and R. Lipperheide, Nucl. Phys. A189, 113 (1972).
[76]A. Aswad *et al.*, Nucl. Phys. A208, 61 (1973).
[77]M. Kirbakh and Kh. U. Eger, Yad. Fiz. 29, 1191 (1979) [Sov. J. Nucl. Phys. 29, 614 (1979)].
[78]H. Tyren *et al.*, Nucl. Phys. 79, 321 (1966).
[79]Kh. R. Kissener and R. A. Éramzhyan, Fiz. Elem. Chastits At. Yadra (to be published).
[80]B. H. Wildenthal *et al.*, Phys. Rev. C 4, 1266, 1708 (1971).
[81]E. A. Eramzhyan and H. R. Kissener, Abstract 1.20 of Contributed Papers at Intern. Conf. on Nuclear Physics with Electromagnetic Interactions, Mainz (1979).
[82]Yu. M. Arkatov *et al.*, Yad. Fiz. 19, 1172 (1974) [Sov. J. Nucl. Phys. 19, 598 (1974)].
[83]J. Ahrens *et al.*, Nucl. Phys. A251, 479 (1975).
[84]N. Bezic *et al.*, Nucl. Phys. A128, 426 (1969).
[85]B. L. Berman, At. Data Nucl. Data Tables 15, 319 (1975).
[86]A. Murakami, J. Phys. Soc. Jpn. 28, 1 (1970).
[87]V. P. Denisov, L. A. Kul'chitskii, I. Ya. Chubukov, Izv. Akad. Nauk SSSR, Ser. Fiz. 37, 107 (1973).
[88]S. Ferroni *et al.*, Nucl. Phys. 76, 58 (1966).
[89]S. C. Fultz *et al.*, Phys. Rev. 143, 790 (1966).
[90]G. G. Taran and A. N. Gorbunov, Zh. Eksp. Teor. Fiz. 46, 1492 (1964) [Sov. Phys. JETP 19, 1010 (1964)].
[91]V. N. Maĭkov, Zh. Eksp. Teor. Fiz. 34, 1406 (1958) [Sov. Phys. JETP 7, 973 (1958)].
[92]J. W. Juri *et al.*, Phys. Rev. C 19, 1684 (1979).
[93]P. S. Fisher *et al.*, Nucl. Phys. 45, 113 (1963).
[94]H. U. Jager, H. R. Kissener, and R. A. Eramzhyan, Nucl. Phys. A171, 584 (1971).
[95]D. J. Albert *et al.*, Phys. Rev. C 16, 503 (1977).
[96]M. H. Harakeh *et al.*, Phys. Rev. C 12, 1410 (1975).
[97]M. A. Zhusupov, V. V. Karapetyan, and R. A. Éramzhyan, Izv. Akad. Nauk SSSR, Ser. Fiz. 33, 730 (1969).
[98]R. F. Fraser, R. K. Garnworthy, and B. M. Spicer, Nucl. Phys. A156, 489 (1970).
[99]H. A. Medicus *et al.*, Nucl. Phys. A156, 257 (1970).
[100]Y. M. Shin, D. M. Skopik, and J. J. Murphy, Phys. Lett. B55, 297 (1975).
[101]G. Junghans *et al.*, Z. Phys. A291, 353 (1979).
[102]S. L. Blatt *et al.*, Phys. Rev. 176, 1147 (1968).
[103]E. Ventura, C. C. Chang, and W. E. Meyerhof, Nucl. Phys. A173, 1 (1971).
[104]A. M. Young, S. L. Blatt, and R. G. Seyler, Phys. Rev. Lett. 25, 1764 (1970); E. Ventura, J. R. Calarco, W. E. Meyerhof, and A. M. Young, Phys. Lett. B46, 364 (1973).
[105]K. Nakamura *et al.*, Nucl. Phys. A296, 431 (1978).
[106]F. Ajzenberg and T. Lauritsen, Nucl. Phys. 78, 22 (1966).
[107]F. Ajzenberg, Nucl. Phys. A320, 31 (1979).
[108]F. P. Brady *et al.*, Phys. Rev. C 16, 31 (1977).

[109]B. R. Wienke and S. L. Meyer, Phys. Rev. C 3, 2179 (1971); 9, 943 (1974).
[110]S. L. Mintz, Phys. Rev. C 19, 476 (1979); 20, 286 (1979).
[111]Yu. A. Batusov *et al.*, Yad. Fiz. 28, 459 (1978) [Sov. J. Nucl. Phys. 28, 233 (1978)].
[112]Yu. M. Volkov *et al.*, Yad. Fiz. 27, 868 (1978) [Sov. J. Nucl. Phys. 27, 461 (1978)].
[113]V. I. Kukulin, V. G. Neudachin, and V. N. Pomerantsev, Yad. Fiz. 24, 298 (1976) [Sov. J. Nucl. Phys. 24, 155 (1976)]; J. Phys. G 4, 1409 (1978); V. I. Kukulin, V. G. Neudachin, and Yu. F. Smirnov, Fiz. Elem. Chastits At. Yadra 10, 1236 (1979) [Sov. J. Part. Nucl. 10, 492 (1979)].
[114]V. P. Denisov and I. Ya. Chubukov, Yad. Fiz. 20, 1106 (1974) [Sov. J. Nucl. Phys. 20, 579 (1975)].
[115]V. P. Denisov, Yad. Fiz. 27, 882 (1978) [Sov. J. Nucl. Phys. 27, 469 (1978)].
[116]A. G. Gregory, T. R. Sherwood, and E. W. Titterton, Nucl. Phys. 32, 543 (1962).
[117]D. M. Skopik, J. Asai, E. L. Tomusiak, and J. J. Murphy, II, Phys. Rev. C 20, 2025 (1979).
[118]B. S. Ishkhanov, V. I. Mokeev, Yu. A. Novikov, and I. M. Piskarev, Yad. Fiz. 32, 11 (1980) [Sov. J. Nucl. Phys. 32, 5 (1980)].
[119]V. P. Denisov and L. A. Kul'chitskiĭ, Yad. Fiz. 5, 490 (1967) [Sov. J. Nucl. Phys. 5, 344 (1967)].
[120]M. K. Leung, J. J. Murphy, J. M. Shin, and D. M. Skopik, Can. J. Phys. 55, 252 (1977).
[121]A. Buchnea, R. G. Johnson, and K. G. McNeill, Can. J. Phys. 56, 47 (1978).
[122]V. P. Denisov and L. A. Kul'chitskiĭ, Yad. Fiz. 3, 268 (1966) [Sov. J. Nucl. Phys. 3, 192 (1966)].
[123]G. Strassner *et al.*, Phys. Rev. C 20, 248 (1979).
[124]A. Goldman and M. Stroetzel, Z. Phys. 239, 235 (1970).
[125]G. J. Vanpraent, Nucl. Phys. 74, 219 (1965).
[126]J. P. Perroud, in: Photopion Nuclear Physics, Plenum Press, New York (1969), p. 69.
[127]P. Truöl, in: Lecture Notes in Physics, Vol. 108, Nuclear Physics with Electromagnetic Interactions, Springer, Berlin (1979).
[128]A. Yamaguchi *et al.*, Phys. Rev. C 3, 1750 (1971).
[129]N. Ensslin *et al.*, Phys. Rev. C 19, 569 (1979).

Translated by Julian B. Barbour